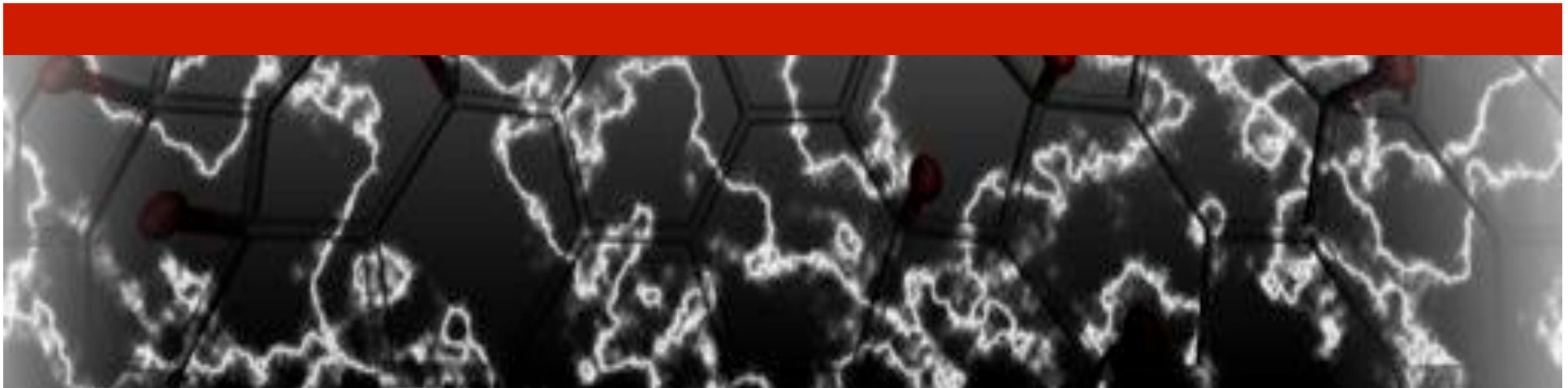


Emergent Electromechanical Properties of Nanoscale Materials

July 1, 2013

Karel-Alexander Duerloo, Mitchell Ong, Yao Li, Evan Reed

*Department of Materials Science and Engineering
Stanford University*



- Some current research themes:
 - 2D materials for electronics and energy
 - Materials at high T, p, and electric fields
 - Semiclassical methods
 - Time-dependent quantum methods
 - Statistical algorithms for big materials data

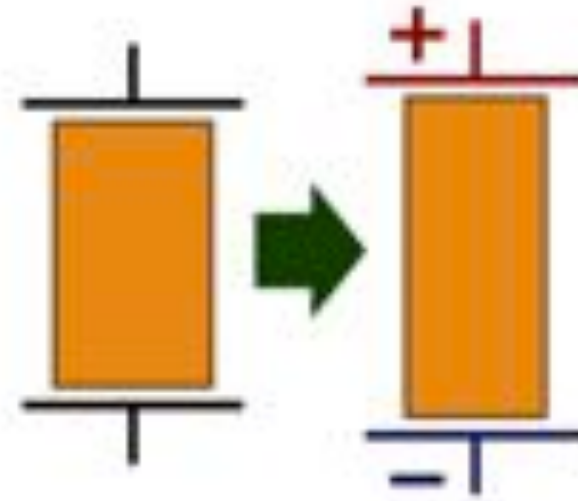


Contact: Evan Reed
evanreed@stanford.edu
<http://www.stanford.edu/~evanreed/>

OUTLINE

- Electromechanical properties of materials:
Piezoelectricity and Flexoelectricity
- Quantum origins of electrical polarization in crystals:
Polarization as a Berry phase
- Kohn-Sham DFT-based calculations to discover
piezoelectric properties of monolayer and few-layer
materials

PIEZOELECTRICITY: THE CARTOON



Mechanical deformation and electric fields are linearly related in piezoelectric crystals.

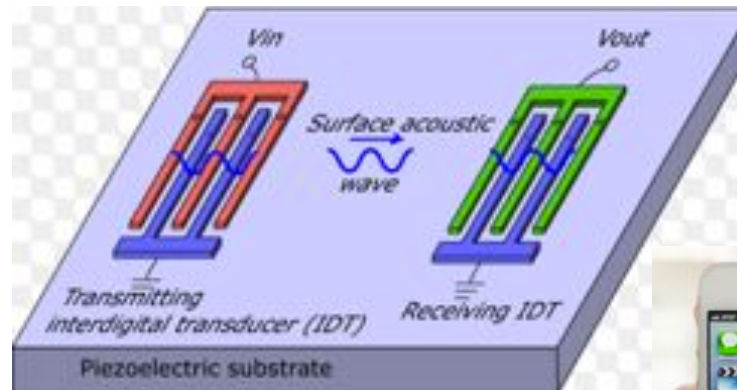
PIEZOELECTRIC MATERIAL APPLICATIONS



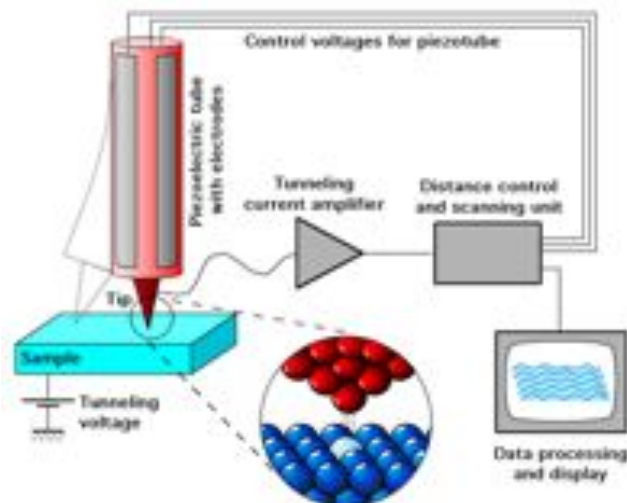
Stress Sensors



Acoustic transducers for signal processing



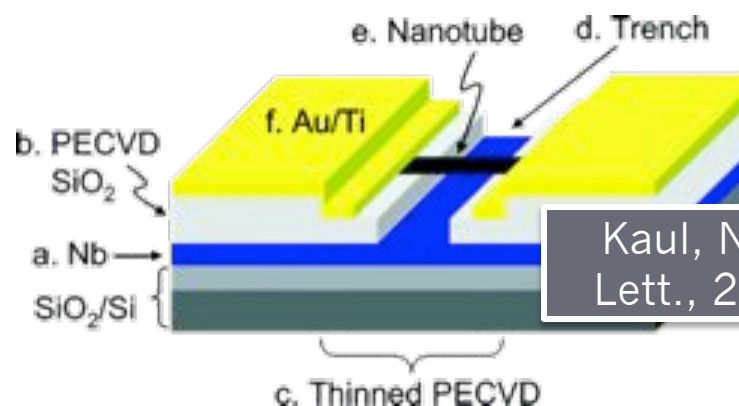
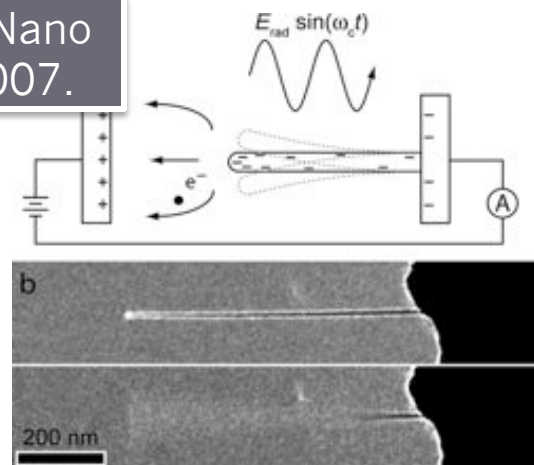
Scanning Tunneling Microscope (STM)



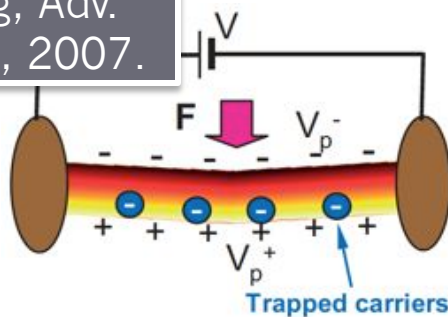
Piezoelectrics can control sub-atomic scale displacements of an STM tip relative to a surface.

electromechanical nanotube devices

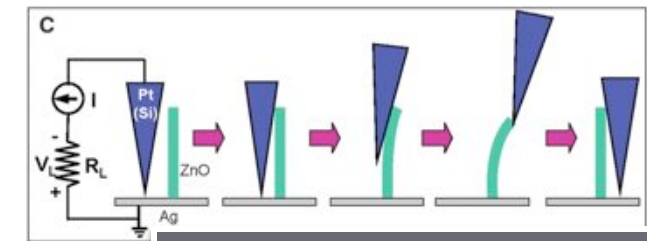
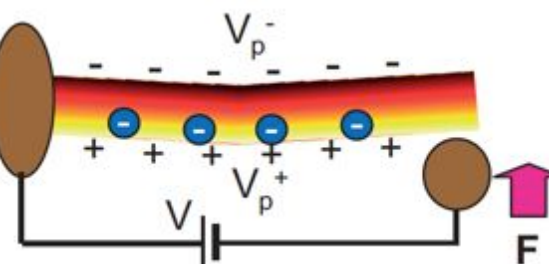
Jensen, Nano Lett., 2007.



Wang, Adv. Mater., 2007.



piezotronic nanowires



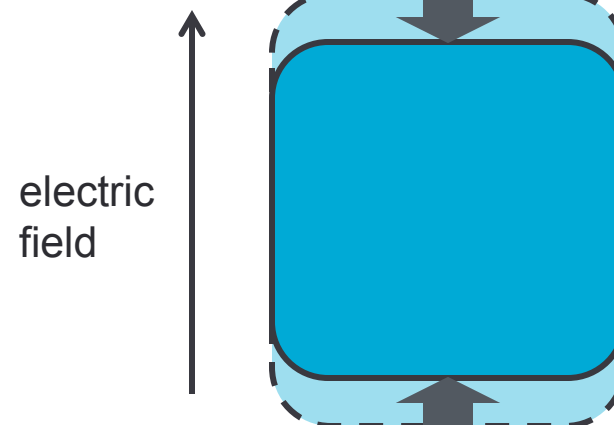
piezoelectric effect

$$P_i = e_{ijk} \epsilon_{jk}$$



converse piezoelectric effect

$$\epsilon_{ij} = d_{ijk} E_k$$



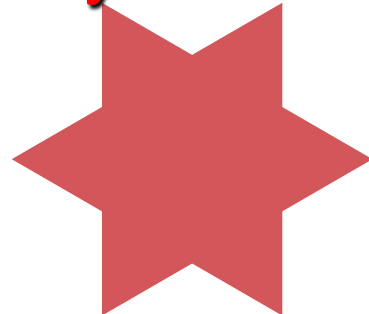
Piezoelectric materials must exhibit:

1. An electronic bandgap
2. A lack of centrosymmetry

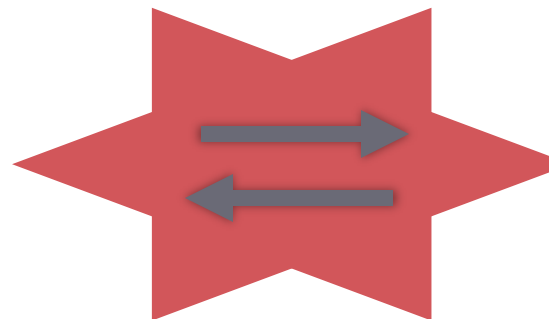
Inversion symmetry of a crystal => $d_{ijk} = (-1)^3 d_{ijk} = -d_{ijk}$
 So $d_{ijk}=0$ for crystals with inversion symmetry!



Centrosymmetric



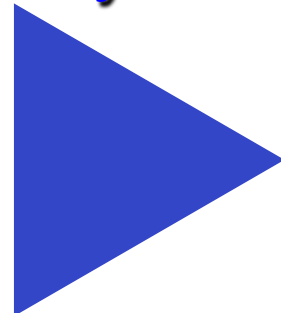
$$\varepsilon_{xx}$$



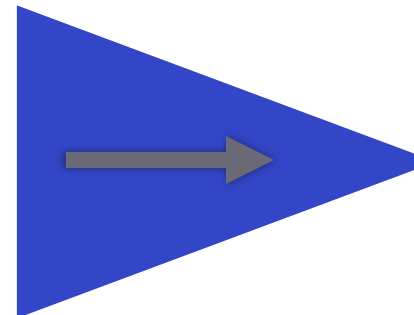
Non-polar.

$$\Delta P = 0.$$

Non-centrosymmetric



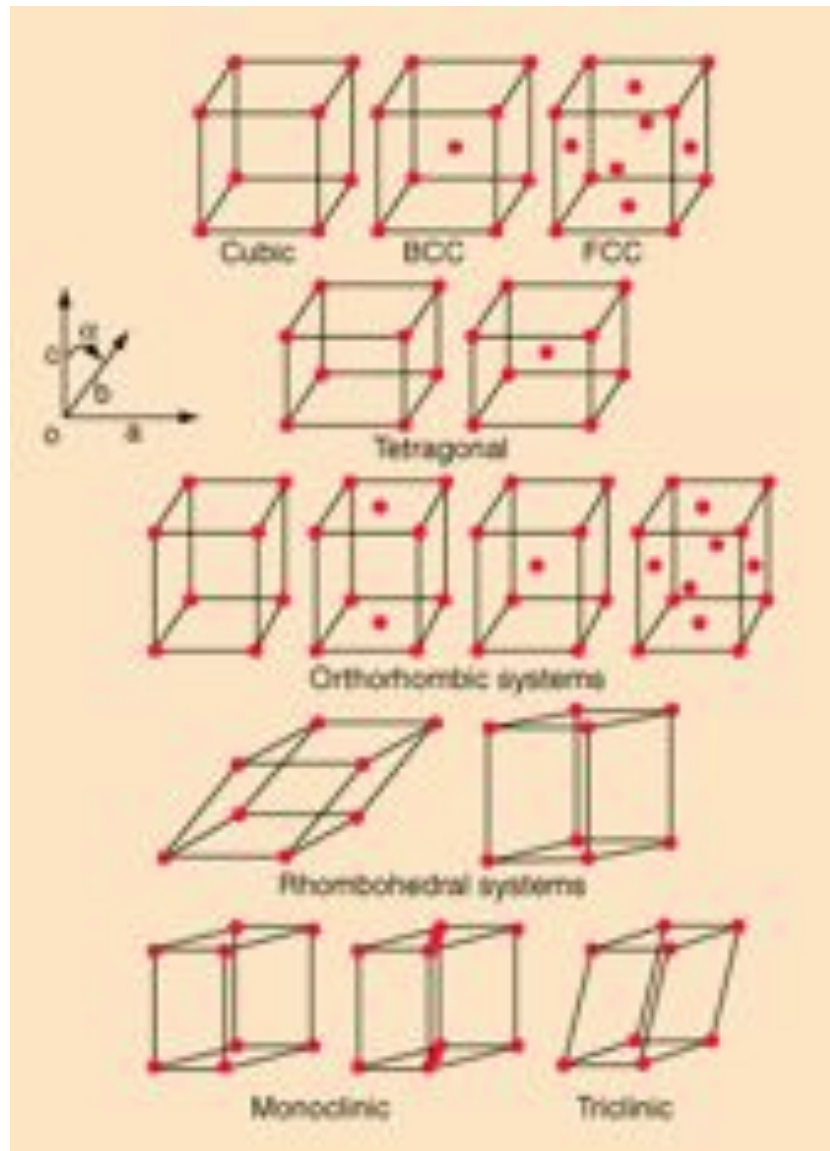
$$\varepsilon_{xx}$$



Polar!

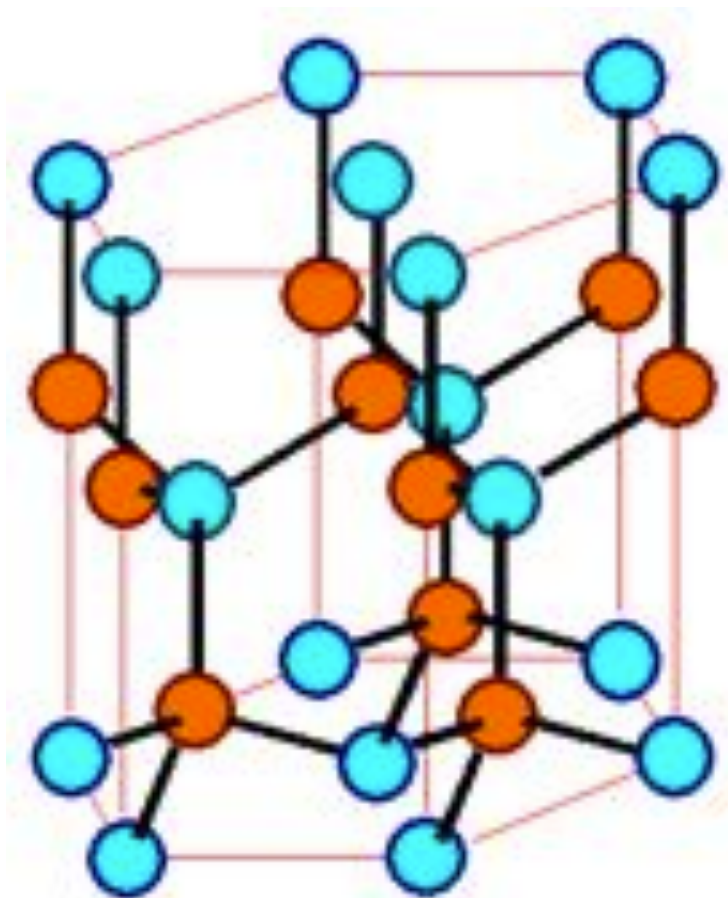
ΔP allowed.

CAN ANY OF THESE CRYSTALS BE PIEZOELECTRIC?

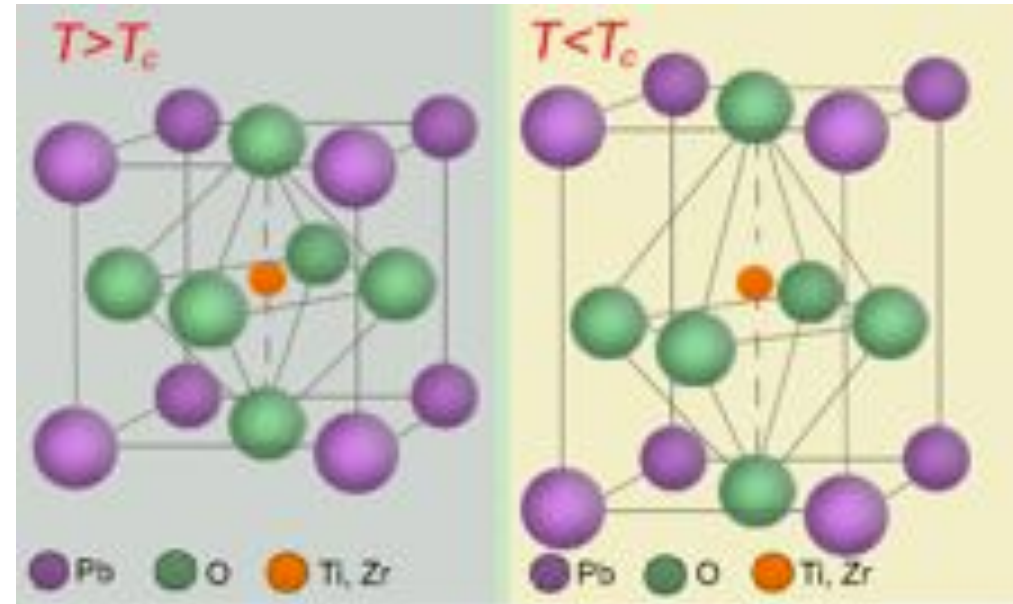


14 Bravais lattices with one atom per lattice point.

Wurtzite structure:
ZnO, GaN, AlN, etc.



Perovskites can be
piezoelectric and *ferroelectric*:
 BaTiO_3 , $\text{PbZr}_x\text{Ti}_{1-x}\text{O}_3$, etc.



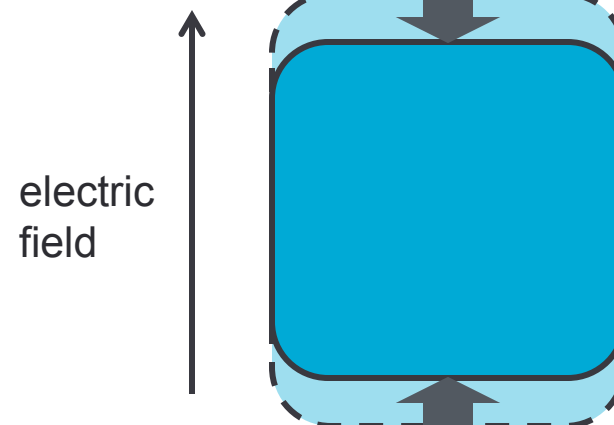
piezoelectric effect

$$P_i = e_{ijk} \epsilon_{jk}$$



converse piezoelectric effect

$$\epsilon_{ij} = d_{ijk} E_k$$



Piezoelectric materials must exhibit:

1. An electronic bandgap
2. A lack of centrosymmetry

Inversion symmetry of a crystal => $d_{ijk} = (-1)^3 d_{ijk} = -d_{ijk}$
 So $d_{ijk} = 0$ for crystals with inversion symmetry!

THE NOBEL PRIZE FOR MANY-ELECTRON QUANTUM METHODS



The Nobel Prize in Chemistry 1998

"for his development of the density-functional theory"

"for his development of computational methods in quantum chemistry"



Walter Kohn

1/2 of the prize

USA



John A. Pople

1/2 of the prize

United Kingdom



FORMAL DFT IS BASED ON TWO INITIAL DEVELOPMENTS



INHOMOGENEOUS ELECTRON GAS

[find it](#) [SU](#) [Print](#) [E-mail](#) [Add to Marked List](#) [Save to EndNote Web](#) [Save to EndNote, RefMan, ProCite](#) [more options](#)

Author(s): HOHENBERG P, KOHN W

Source: PHYSICAL REVIEW B Volume: 136 Issue: 3B Pages: B864-& Published: 1964

Times Cited: 7,100 References: 16

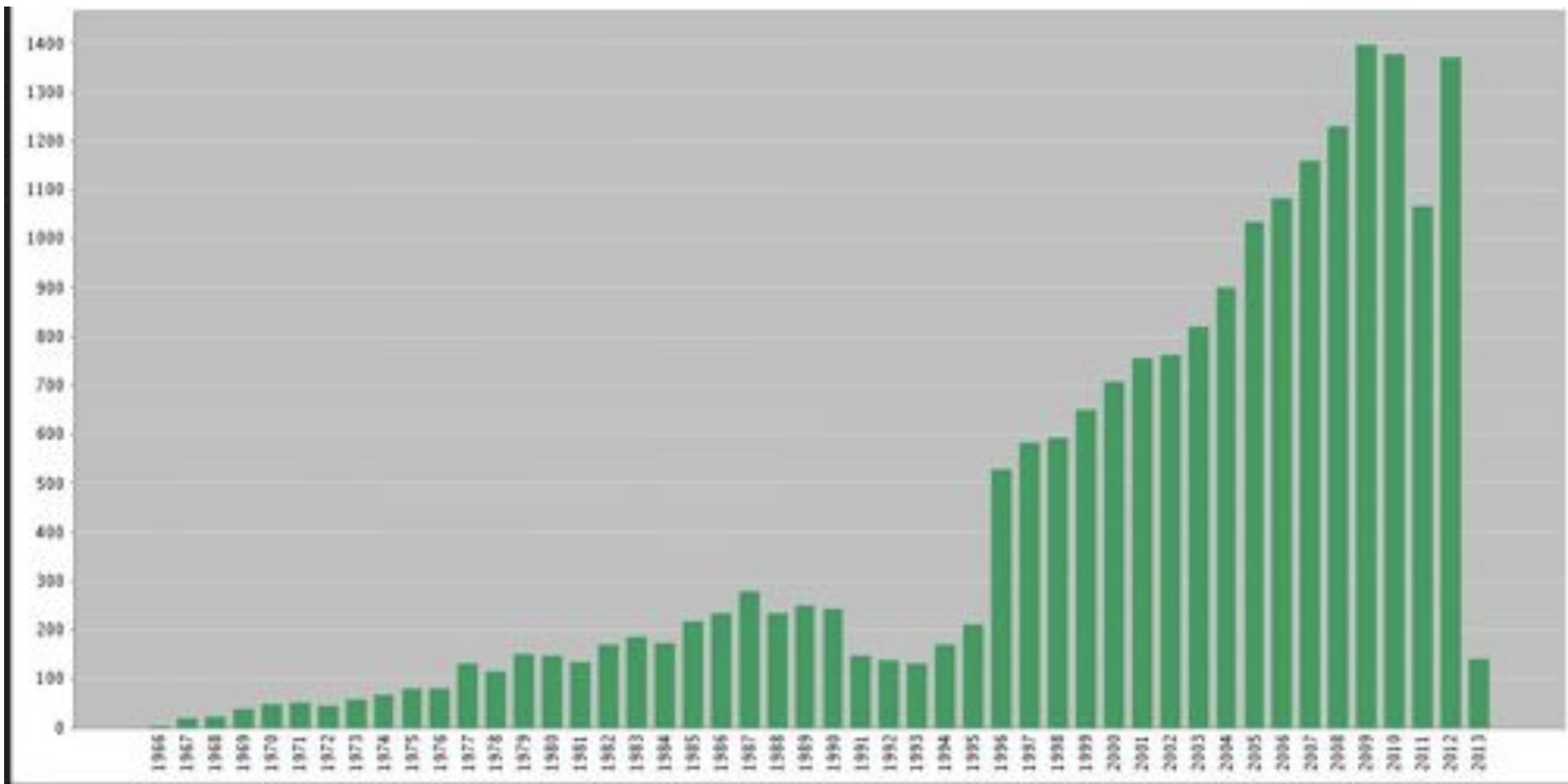
SELF-CONSISTENT EQUATIONS INCLUDING EXCHANGE AND CORRELATION EFFECTS

[find it](#) [SU](#) [Print](#) [E-mail](#) [Add to Marked List](#) [Save to EndNote Web](#) [Save to EndNote, RefMan, ProCite](#) [more options](#)

Author(s): KOHN W, SHAM LJ

Source: PHYSICAL REVIEW Volume: 140 Issue: 4A Pages: 1133-& Published: 1965

Times Cited: 16,206 References: 13



SELF-CONSISTENT EQUATIONS INCLUDING EXCHANGE AND CORRELATION EFFECTS

find it SU

[Print](#) [E-mail](#) [Add to Marked List](#) [Save to EndNote Web](#) [Save to EndNote, RefMan, ProCite](#) [more options](#)

Author(s): KOHN W, SHAM LJ

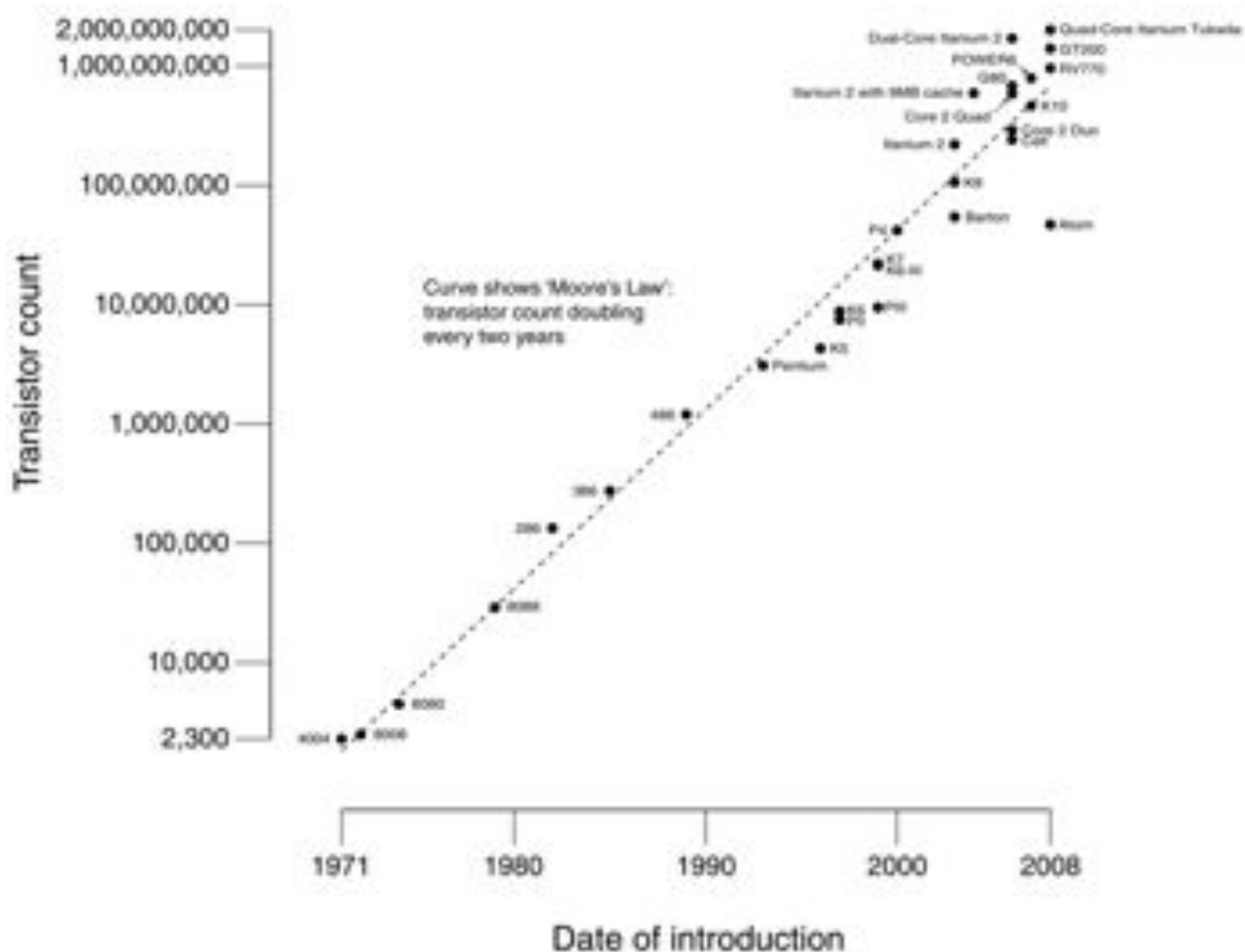
Source: PHYSICAL REVIEW Volume: 140 Issue: 4A Pages: 1133-& Published: 1965

Times Cited: 16,206 References: 13

Citation Map

Walter J. Roush
Based on Density Functional Theory
modeling
Evan Reed
Stanford University

CPU Transistor Counts 1971-2008 & Moore's Law





Hohenberg Kohn theorem

For the ground electronic state, there is a one to one correspondence between the electron density and the total energy, $E_{\text{total}} = E[\rho(\vec{r})]$.

Therefore, finding the ground state energy of a many-body system boils down to finding the density $\rho(\vec{r})$ that minimizes $E[\rho(\vec{r})]$.

Profound feature: Calculation of wavefunctions is not required!

The form of the potential $V_{\text{nuc}}(\vec{r})$ (determined by the electron - nuclear interactions) uniquely determines the electron density $\rho(\vec{r})$. Note that the other terms in the Hamiltonian are universal.



HOHENBERG AND KOHN, 1964



- The information content in the many body wavefunction ($\sim N_{\text{mesh_points}}^{N_{\text{electrons}}}$) is far greater than the single particle density ($\sim N_{\text{mesh_points}}$), so a LOT of information is being lost by working only with the density!
- Naively, one might think that all that extra information is required to determine the ground state energy

A universal density functional for materials (Hohenberg and Kohn)

$$\begin{aligned}E[\rho(\vec{r})] &= \langle \psi | \mathcal{H} | \psi \rangle \\&= \langle \psi | T + V_{\text{nuc}} + W | \psi \rangle \\&= \langle \psi | T + W | \psi \rangle + \int d\vec{r} \rho(\vec{r}) V_{\text{nuc}}(\vec{r}) \\&= F[\rho(\vec{r})] + \int d\vec{r} \rho(\vec{r}) V_{\text{nuc}}(\vec{r})\end{aligned}$$

where T contains the kinetic energy terms and W contains the electron-electron interaction terms. The functional $F[\rho(\vec{r})]$ is independent of the external potential and is universal in nature.

$$F[\rho(\vec{r})] = T[\rho(\vec{r})] + W[\rho(\vec{r})]$$

A snag in the quest for density-centric glory: $T[\rho(\vec{r})]$

How can $T[\rho(\vec{r})]$ be evaluated? It requires the exact many-body wavefunctions...



Kohn and Sham proposed an alternative scheme: Use fictitious single-particle, uncorrelated electron states $\phi_\ell(\vec{r})$ (in Hartree-Fock or similar form) that give the same total density $\rho(\vec{r})$ as the exact many-body state. Then,

$$T[\rho(\vec{r})] \approx T_s[\rho(\vec{r})] = \sum_\ell \langle \phi_\ell | -\frac{\hbar^2}{2m} \nabla^2 | \phi_\ell \rangle$$

Introduction of the exchange-correlation functional

Using Kohn-Sham states,

$$\begin{aligned} E[\rho(\vec{r})] &= T[\rho(\vec{r})] + W[\rho(\vec{r})] + \int d\vec{r} \rho(\vec{r}) V_{\text{nuc}}(\vec{r}) \\ &= T_s[\rho(\vec{r})] + E_{\text{Hartree}}[\rho(\vec{r})] + \int d\vec{r} \rho(\vec{r}) V_{\text{nuc}}(\vec{r}) \\ &\quad + (T[\rho(\vec{r})] - T_s[\rho(\vec{r})] + W[\rho(\vec{r})] - E_{\text{Hartree}}[\rho(\vec{r})]) \\ &= T_s[\rho(\vec{r})] + E_{\text{Hartree}}[\rho(\vec{r})] + \int d\vec{r} \rho(\vec{r}) V_{\text{nuc}}(\vec{r}) + E_{\text{XC}}[\rho(\vec{r})] \end{aligned}$$

Here, the exchange-correlation functional $E_{\text{XC}}[\rho(\vec{r})]$ is primarily composed of the electronic exchange and correlation energy. We could include exact exchange in the Hartree-Fock fashion (and DFT some approaches do), but let's lump it into $E_{\text{XC}}[\rho(\vec{r})]$ for now.

Kohn-Sham DFT

We have arrived at Kohn-Sham DFT, the most commonly employed form:

$$\left[\frac{-\hbar^2 \nabla^2}{2m} + V_{nuc}(\vec{r}) + \sum_j \int d\vec{r}' \frac{\phi_j(\vec{r}')^* \phi_j(\vec{r}')}{|\vec{r} - \vec{r}'|} + \frac{\delta E_{XC}[\rho(\vec{r})]}{\delta \rho(\vec{r})} \right] \phi_i(\vec{r}) = \epsilon_i \phi_i(\vec{r})$$

where $\frac{\delta E_{XC}[\rho(\vec{r})]}{\delta \rho(\vec{r})}$ is the exchange-correlation potential, typically determined with some empiricism.

Comparison between KS DFT and Hartree-Fock

Note the close similarity between the single particle equations for KS-DFT:

$$\left[\frac{-\hbar^2 \nabla^2}{2m} + V_{nuc}(\vec{r}) + \sum_j \int d\vec{r}' \frac{\phi_j(\vec{r}')^* \phi_j(\vec{r}')}{|\vec{r} - \vec{r}'|} + \frac{\delta E_{XC}[\rho(\vec{r})]}{\delta \rho(\vec{r})} \right] \phi_i(\vec{r}) = \epsilon_i \phi_i(\vec{r})$$

and HF:

$$\begin{aligned} & \left[\frac{-\hbar^2 \nabla^2}{2m} + V_{nuc}(\vec{r}) + \sum_j \int d\vec{r}' \frac{\phi_j(\vec{r}')^* \phi_j(\vec{r}')}{|\vec{r} - \vec{r}'|} \right] \phi_i(\vec{r}) \\ & - \sum_j \int d\vec{r}' \frac{\phi_j(\vec{r}')^* \phi_i(\vec{r}')}{|\vec{r} - \vec{r}'|} \phi_j(\vec{r}) \delta_{s_i s_j} = \epsilon_i \phi_i(\vec{r}) \end{aligned}$$

Could the KS-DFT approach be empirically arrived at from HF equations?



Suppose the potential $V(\vec{r})$ has translational periodicity $V(\vec{r} + \vec{R}) = V(\vec{r})$ where $\vec{R} = \ell\vec{a}_1 + m\vec{a}_2 + n\vec{a}_3$ is a linear combination of lattice vectors \vec{a} . The eigenstates of the Hamiltonian with such a potential have the form,

$$\psi_{\vec{k}}(\vec{r}) = e^{i\vec{k}\cdot\vec{r}} u_{\vec{k}}(\vec{r})$$

where

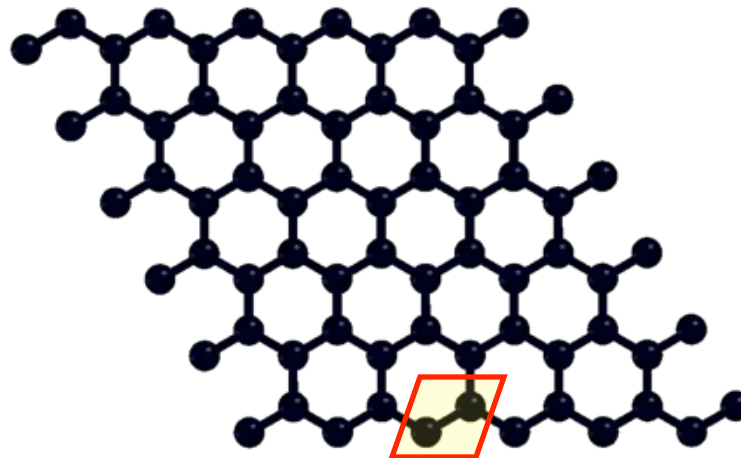
$$u_{\vec{k}}(\vec{r} + \vec{R}) = u_{\vec{k}}(\vec{r})$$

The function $u_{\vec{k}}(\vec{r})$ has the periodicity of the lattice.

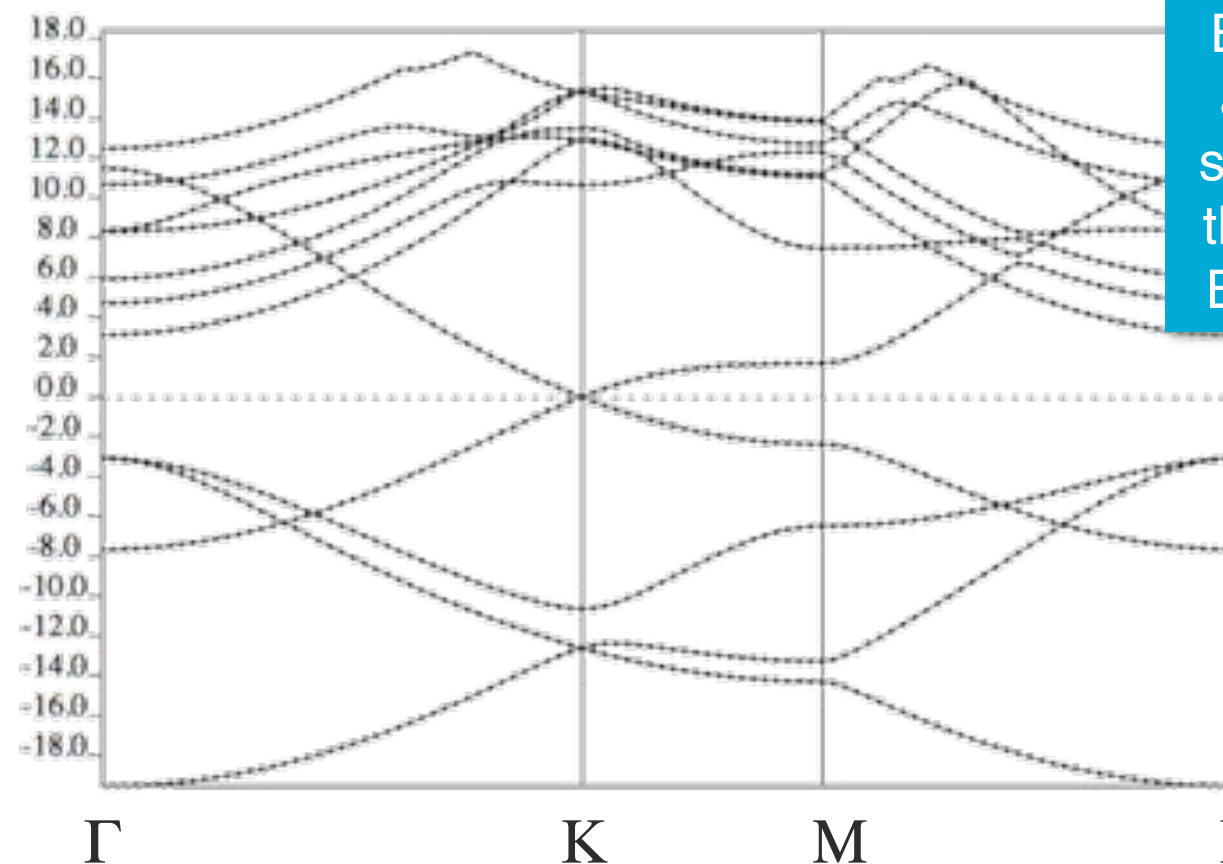
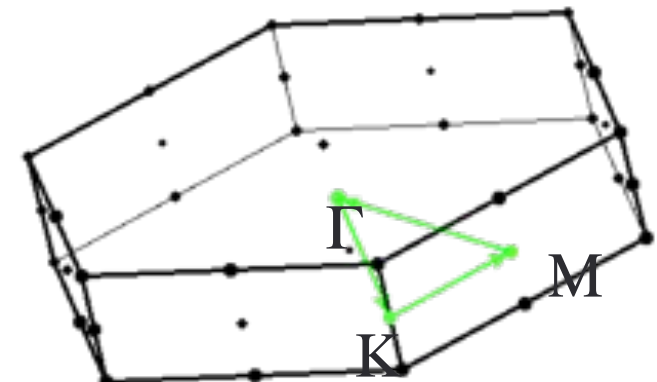
BLOCH STATES DESCRIBE ELECTRONS IN A CRYSTAL



- ▶ For a bulk material, the quantum number \vec{k} can be considered a continuous variable.
- ▶ There are a total of two quantum numbers for that describe such periodic states: \vec{k} and n . $\psi_{\vec{k},n}(\vec{r})$
- ▶ Note that for QM calculations on a crystal using a computational cell with periodic boundary conditions, the periodicity of the potential $V(\vec{r})$ is the periodicity of the **computational cell** rather than the periodicity of the lattice.
- ▶ All calculations with periodic boundary conditions will exhibit solutions characterized by a quantum number \vec{k} , even liquids, amorphous materials, surfaces, etc.



Graphene



Bands plotted along a high-symmetry path through the 1st Brillouin zone.

The BZ exhibits the point group symmetry of the crystal lattice.



COMPUTATION OF PIEZOELECTRIC COEFFICIENTS



PHYSICAL REVIEW B

VOLUME 47, NUMBER 3

RAPID COMMUNICATIONS

15 JANUARY 1993-I

Theory of polarization of crystalline solids

R. D. King-Smith and David Vanderbilt

Department of Physics and Astronomy, Rutgers University, P. O. Box 849, Piscataway, New Jersey 08855-0849

(Received 10 June 1992)

Absolute polarization of a crystal is ill-defined, but *changes* in polarization are well-defined: $\Delta P_i = e_{ijk} \varepsilon_{jk}$



COMPUTATION OF PIEZOELECTRIC COEFFICIENTS



PHYSICAL REVIEW B

VOLUME 47, NUMBER 3

RAPID COMMUNICATIONS

15 JANUARY 1993-I

Theory of polarization of crystalline solids

R. D. King-Smith and David Vanderbilt

Department of Physics and Astronomy, Rutgers University, P. O. Box 849, Piscataway, New Jersey 08855-0849

(Received 10 June 1992)

Change in polarization due to adiabatic (slow, isentropic) change in strain of computational cell (represented by lambda):

$$\frac{\partial P_\alpha}{\partial \lambda} = -\frac{iq_e\hbar}{N\Omega m_e} \sum_{\mathbf{k}} \sum_{n=1}^M \sum_{m=M+1}^{\infty} \frac{\langle \psi_{\mathbf{k}n}^{(\lambda)} | \hat{p}_\alpha | \psi_{\mathbf{k}m}^{(\lambda)} \rangle \langle \psi_{\mathbf{k}m}^{(\lambda)} | \partial V_{KS}^{(\lambda)} / \partial \lambda | \psi_{\mathbf{k}n}^{(\lambda)} \rangle}{(\epsilon_{\mathbf{k}n}^{(\lambda)} - \epsilon_{\mathbf{k}m}^{(\lambda)})^2} + \text{c.c.}$$

Change in polarization under adiabatic change in strain (from Resta):

$$\Delta \mathbf{P} = \int_0^1 (\partial \mathbf{P} / \partial \lambda) d\lambda$$

$$\Delta \mathbf{P} = \mathbf{P}^{(1)} - \mathbf{P}^{(0)}$$



COMPUTATION OF PIEZOELECTRIC COEFFICIENTS



PHYSICAL REVIEW B

VOLUME 47, NUMBER 3

RAPID COMMUNICATIONS

15 JANUARY 1993-I

Theory of polarization of crystalline solids

R. D. King-Smith and David Vanderbilt

Department of Physics and Astronomy, Rutgers University, P. O. Box 849, Piscataway, New Jersey 08855-0849

(Received 10 June 1992)

After the dust settles:

$$\mathbf{P}^{(\lambda)} = (f q_e / \Omega) \sum_{n=1}^M \int \mathbf{r} |W_n^{(\lambda)}(\mathbf{r})|^2 d\mathbf{r}$$

Wannier function:

$$W_n^{(\lambda)}(\mathbf{r} - \mathbf{R}) = (\sqrt{N} \Omega / 8\pi^3) \int_{BZ} d\mathbf{k} e^{i\mathbf{k} \cdot (\mathbf{r} - \mathbf{R})} u_{\mathbf{k}n}^{(\lambda)}(\mathbf{r})$$

Periodic part of Bloch function:

$$u_{\mathbf{k}n}^{(\lambda)}(\mathbf{r}) = (1/\sqrt{N}) \sum_{\mathbf{R}} e^{-i\mathbf{k} \cdot (\mathbf{r} - \mathbf{R})} W_n^{(\lambda)}(\mathbf{r} - \mathbf{R})$$

Simple interpretation of change in electronic polarization: Change in Wannier center locations.

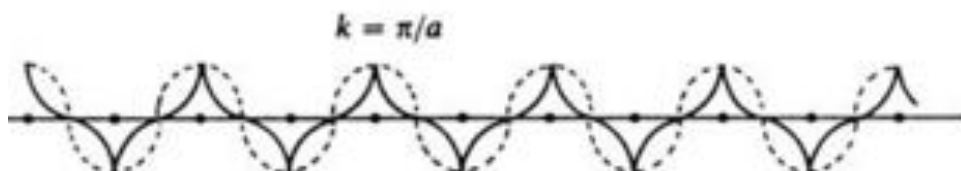
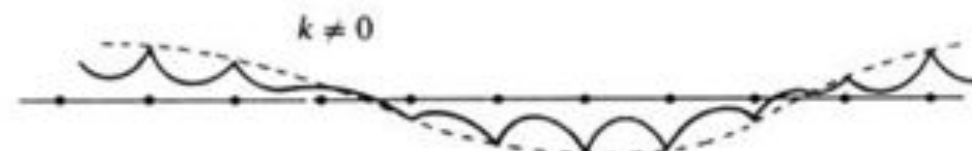
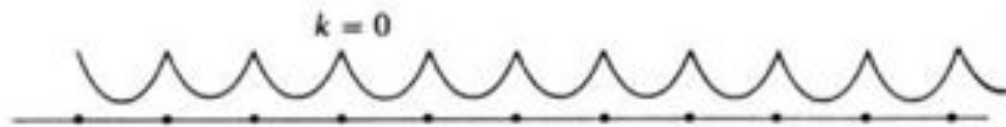
WANNIER FUNCTION: LOCALIZED FT OF EXTENDED BLOCH STATE



Bloch states are extended:

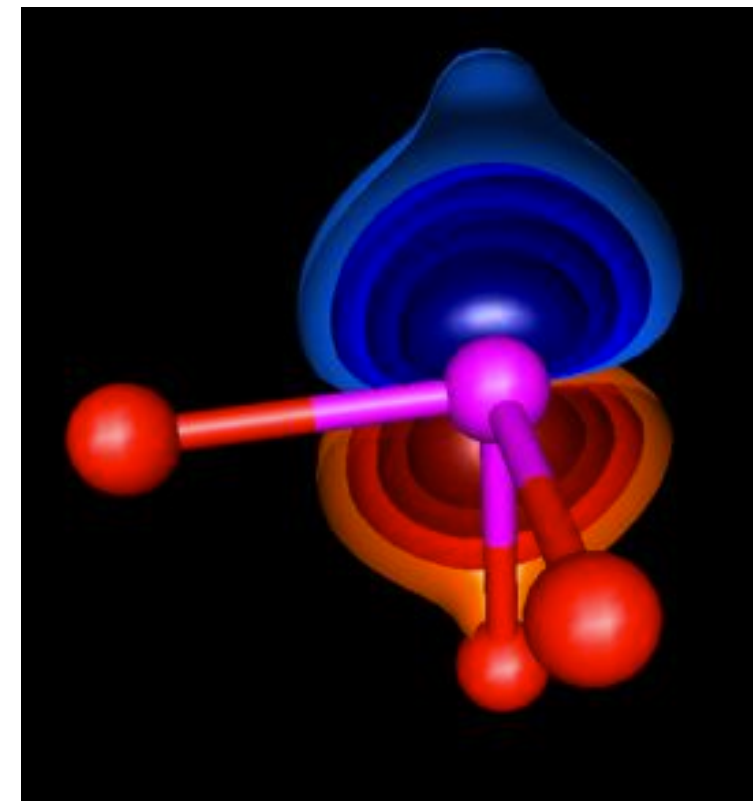
$$\psi_{\vec{k}}(\vec{r}) = e^{i\vec{k} \cdot \vec{r}} u_{\vec{k}}(\vec{r})$$

$$u_{\mathbf{k}n}^{(\lambda)}(\mathbf{r}) = (1/\sqrt{N}) \sum_{\mathbf{R}} e^{-i\mathbf{k} \cdot (\mathbf{r}-\mathbf{R})} W_n^{(\lambda)}(\mathbf{r}-\mathbf{R})$$

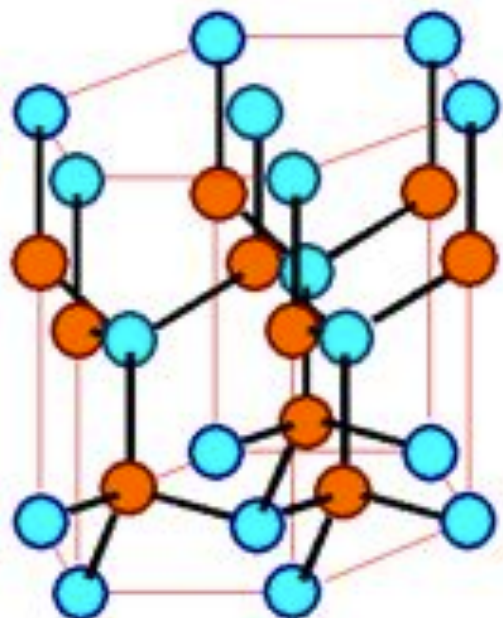


Wannier functions are localized:

$$W_n^{(\lambda)}(\mathbf{r}-\mathbf{R}) = (\sqrt{N} \Omega / 8\pi^3) \int_{BZ} d\mathbf{k} e^{i\mathbf{k} \cdot (\mathbf{r}-\mathbf{R})} u_{\mathbf{k}n}^{(\lambda)}(\mathbf{r})$$



BaTiO_3



Piezoelectric Coefficients

GaN	DFT	Experiment
d_{31} (pm/V)	-1.6	-1.0
e_{31} (C/m ²)	-0.45	-0.55

K. Shimada, *Jpn. J. Appl. Phys.* 45, L358-L360 (2006).

GRAPHENE

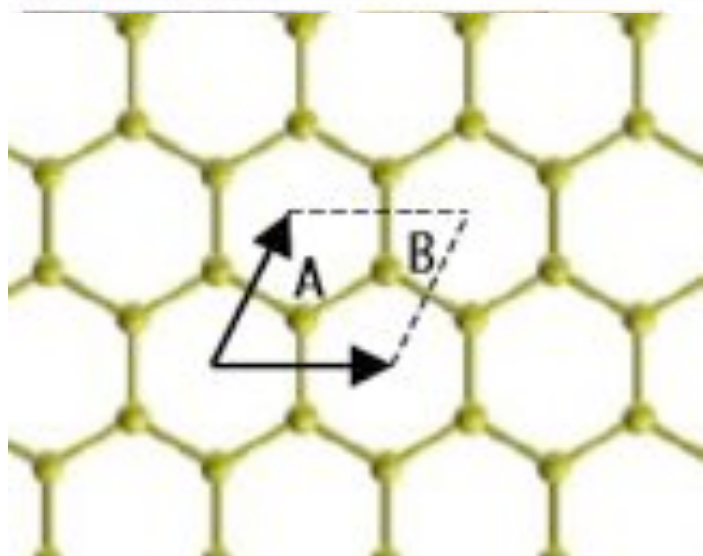


The Nobel Prize in Physics 2010
Andre Geim, Konstantin Novoselov

The Nobel Prize in Physics 2010

Andre Geim

Konstantin Novoselov



The Nobel Prize in Physics 2010 was awarded jointly to Andre Geim and Konstantin Novoselov "for groundbreaking experiments regarding the two-dimensional material graphene".

Geim and Novoselov, Nat. Mat. 6, 183 (2007).

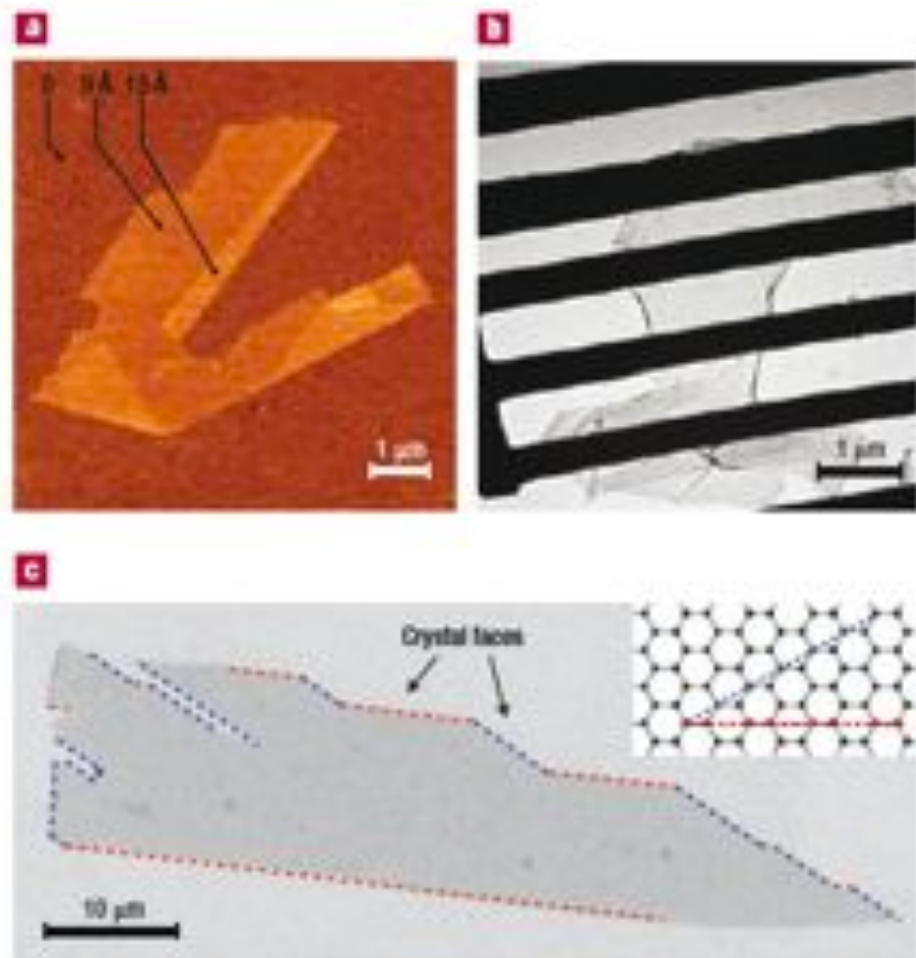
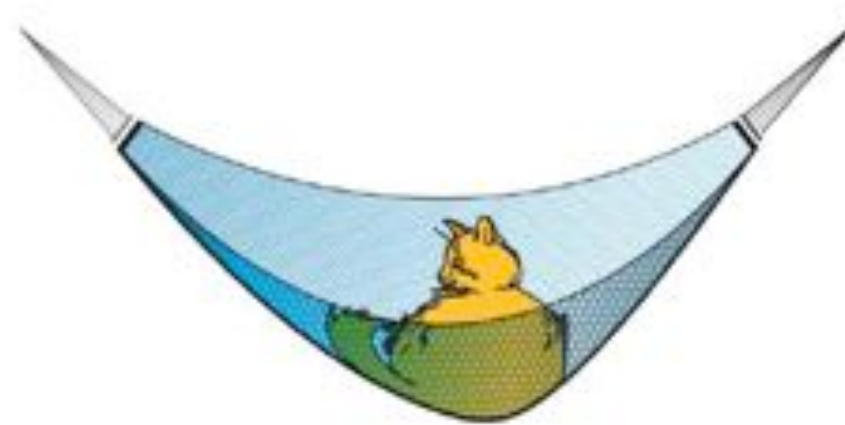
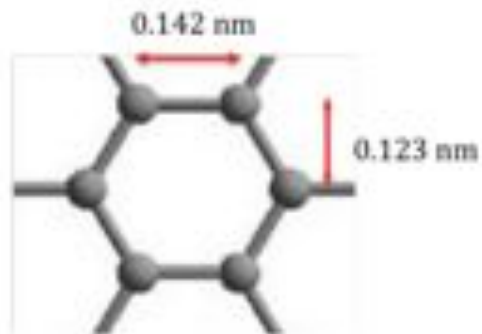


Figure 2 One-atom-thick single crystals: the thinnest material you will ever see. **a**, Graphene visualized by atomic force microscopy (adapted from ref. 8). The folded region exhibiting a relative height of ~ 4 Å clearly indicates that it is a single layer. (Copyright National Academy of Sciences, USA.) **b**, A graphene sheet freely suspended on a micrometre-size metallic scaffold. The transmission electron microscopy image is adopted from ref. 18. **c**, Scanning electron micrograph of a relatively large graphene crystal, which shows that most of the crystal's faces are zigzag and armchair edges as indicated by blue and red lines and illustrated in the inset (T.J. Booth, K.S.N., P. Blake and A.K.G. unpublished work). 10 transport along zigzag edges and edge-related magnetism are expected to attract significant attention.

GRAPHENE'S ANOMALOUS PROPERTIES



Density of graphene

The unit hexagonal cell of graphene contains two carbon atoms and has an area of 0.052 nm^2 . We can thus calculate its density as being 0.77 mg/m^2 . A hypothetical hammock measuring 1m^2 made from graphene would thus weigh 0.77 mg .

Optical transparency of graphene

Graphene is almost transparent, it absorbs only 2.3% of the light intensity, independent of the wavelength in the optical domain. This number is given by $\pi \alpha$, where α is the fine structure constant. Thus suspended graphene does not have any color.

Royal Swedish Academy of Sciences (2010).

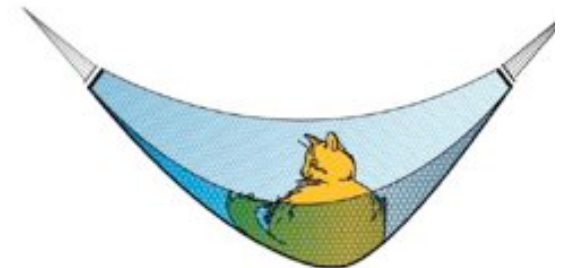
GRAPHENE'S ANOMALOUS PROPERTIES



Strength of graphene

Graphene has a breaking strength of 42N/m. Steel has a breaking strength in the range of 250-1200 MPa= $0.25\text{--}1.2 \times 10^9 \text{ N/m}^2$. For a hypothetical steel film of the same thickness as graphene (which can be taken to be $3.35\text{\AA}=3.35 \times 10^{-10} \text{ m}$, i.e. the layer thickness in graphite), this would give a 2D breaking strength of $0.084\text{--}0.40 \text{ N/m}$. Thus graphene is more than 100 times stronger than the strongest steel.

In our 1 m^2 hammock tied between two trees you could place a weight of approximately 4 kg before it would break. It should thus be possible to make an almost invisible hammock out of graphene that could hold a cat without breaking. The hammock would weigh less than one mg, corresponding to the weight of one of the cat's whiskers.



Electrical conductivity of graphene

The sheet conductivity of a 2D material is given by $\sigma = en\mu$. The mobility is theoretically limited to $\mu=200,000 \text{ cm}^2\text{V}^{-1}\text{s}^{-1}$ by acoustic phonons at a carrier density of $n=10^{12} \text{ cm}^{-2}$. The 2D sheet resistivity, also called the resistance per square, is then 31Ω . Our fictional hammock measuring 1m^2 would thus have a resistance of 31Ω .

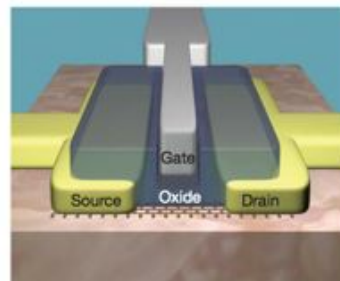
Using the layer thickness we get a bulk conductivity of $0.96 \times 10^6 \Omega^{-1}\text{cm}^{-1}$ for graphene. This is somewhat higher than the conductivity of copper which is $0.60 \times 10^6 \Omega^{-1}\text{cm}^{-1}$.

Thermal conductivity

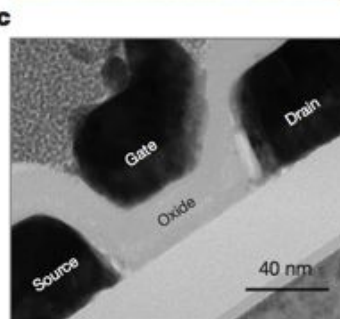
The thermal conductivity of graphene is dominated by phonons and has been measured to be approximately $5000 \text{ Wm}^{-1}\text{K}^{-1}$. Copper at room temperature has a thermal conductivity of $401 \text{ Wm}^{-1}\text{K}^{-1}$. Thus graphene conducts heat 10 times better than copper.

Royal Swedish Academy of Sciences (2010).

MONOLAYER AND FEW-LAYER DEVICES ARE WIDELY VARIED

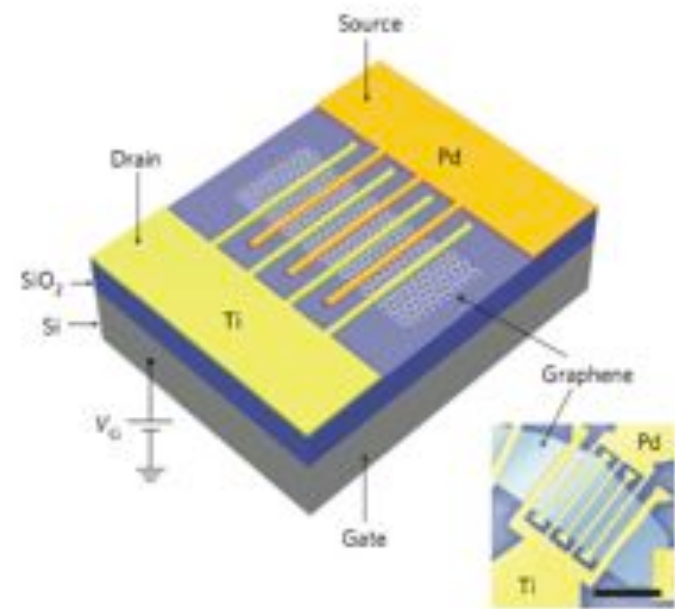


Transistors

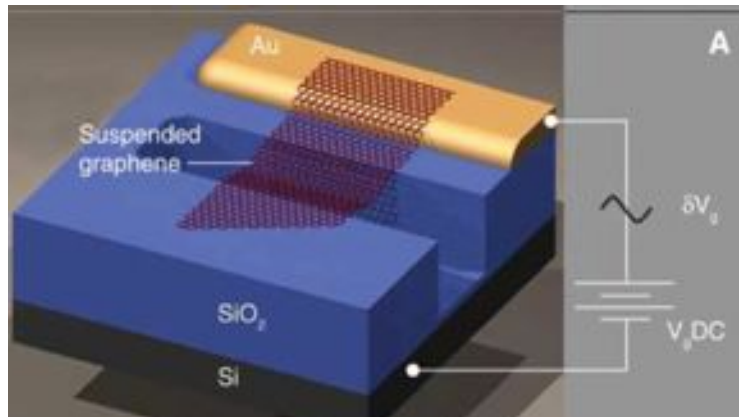


Wu, et al, Nat. 472, 74 (2011).

Photodetectors

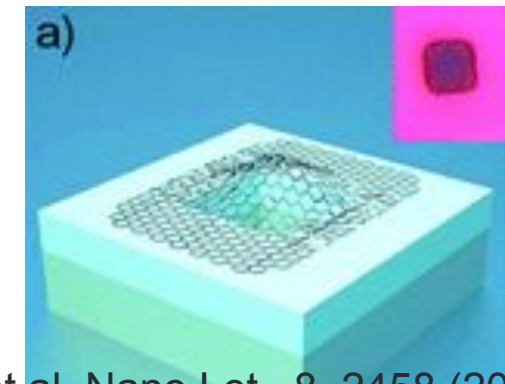


Mechanical resonators



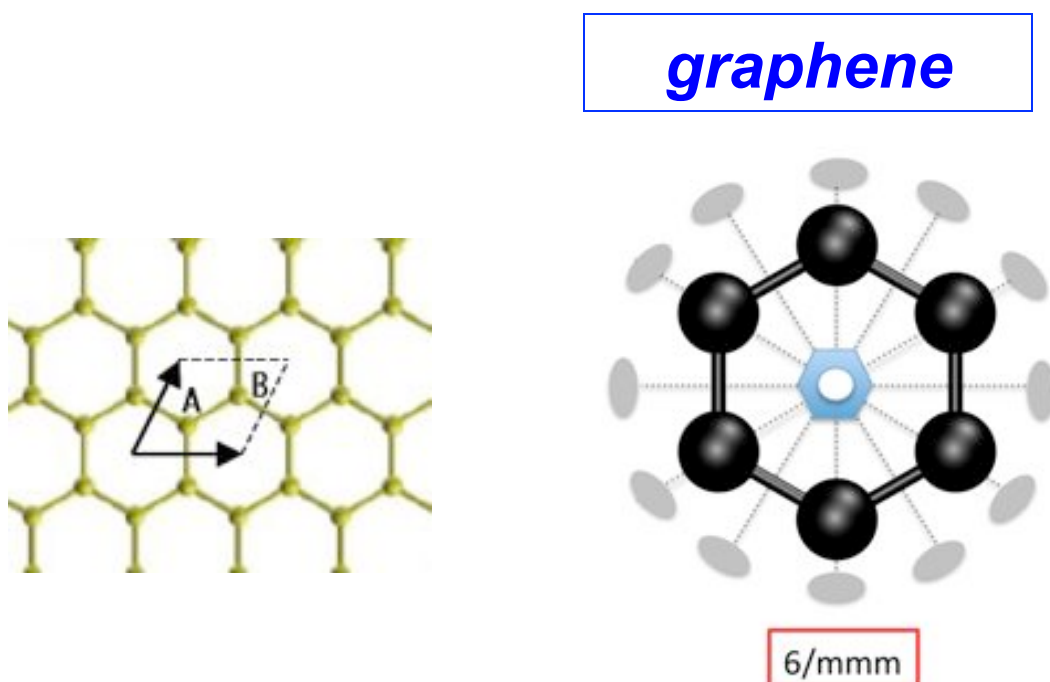
Bunch, et al, Science 315, 490 (2007).

Nanoscale gas confinement

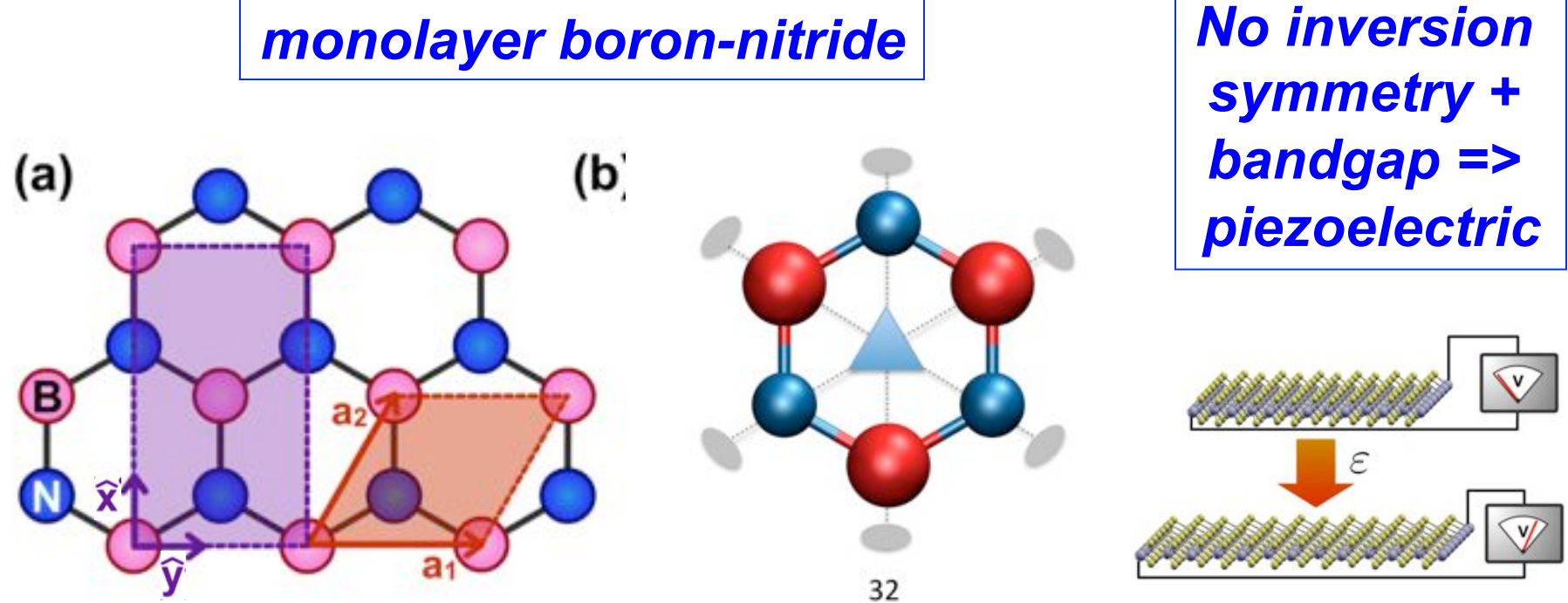


Bunch, et al, Nano Lett. 8, 2458 (2008).

- ★ Nanoscale control can be established by applying voltages across piezoelectric materials (e.g. in STM devices) but graphene is not intrinsically piezoelectric



- *Inversion symmetry => non-piezoelectric*
- *Semi-metallic character => non-piezoelectric*



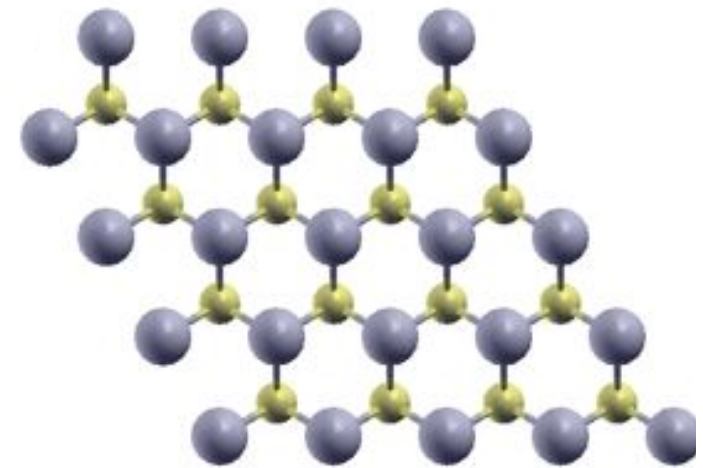
Our (Berry-phase) DFT calculations give $d_{11}=0.6 \text{ pm/V}$.

For comparison:
 Quartz: $d_{11}=2 \text{ pm/V}$
 GaN: $d_{33}=3 \text{ pm/V}$
 PZT: $d_{33} \sim 300 \text{ pm/V}$

$$\begin{bmatrix} \varepsilon_{xx} \\ \varepsilon_{yy} \\ \varepsilon_{xy} \end{bmatrix} = \begin{bmatrix} d_{11} & 0 & 0 \\ -d_{11} & 0 & 0 \\ 0 & -d_{11} & 0 \end{bmatrix} \begin{bmatrix} E_x \\ E_y \\ E_z \end{bmatrix}$$

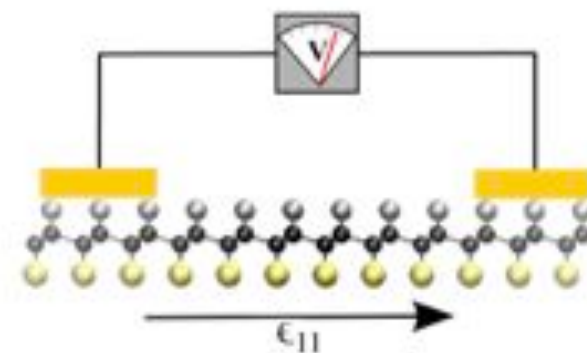
Transition Metal Dichalcogenides: MoS_2 , MoSe_2 , MoTe_2 , WS_2 , WSe_2 , WTe_2

View from above (trigonal prismatic structure):

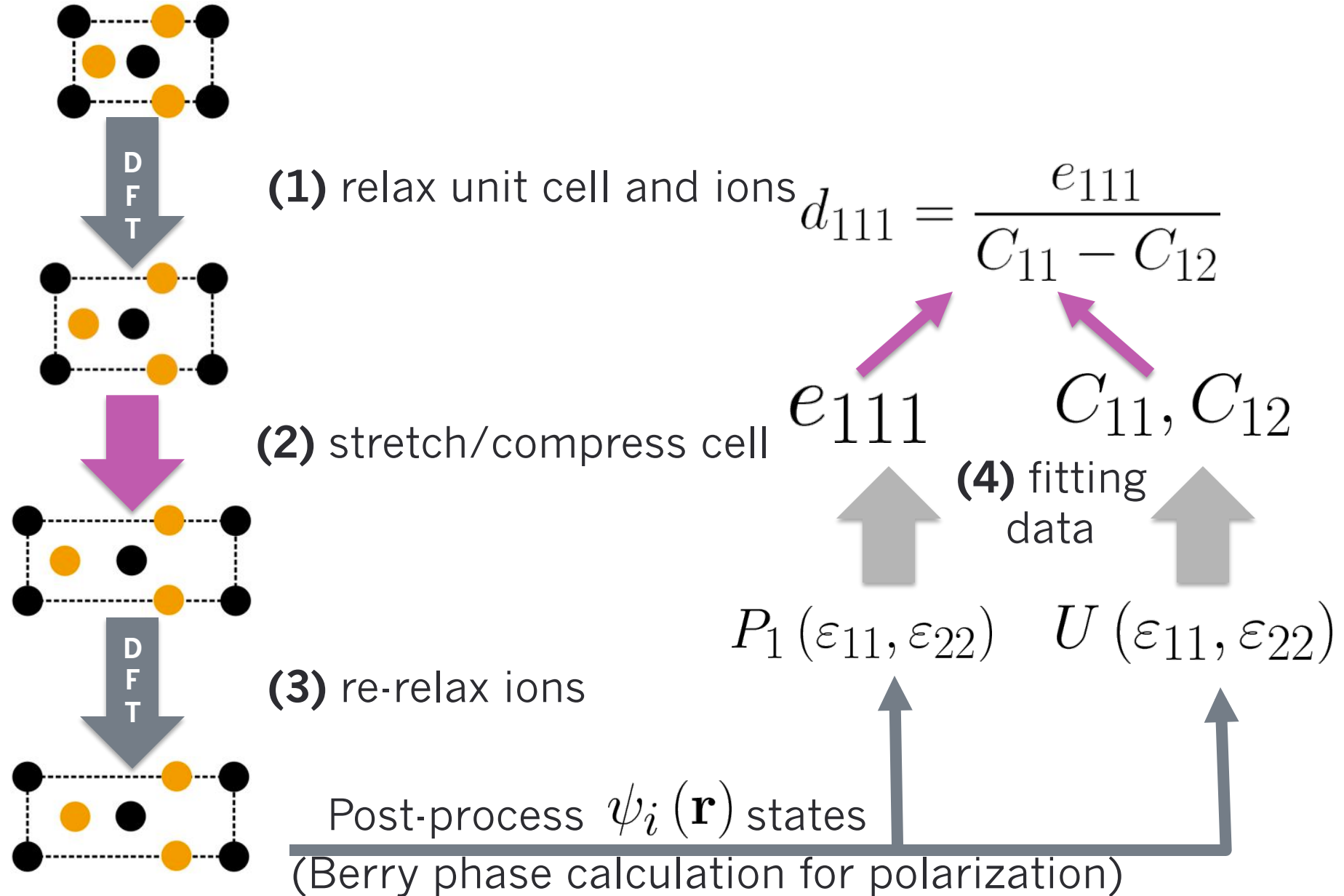


- ✓ **Semiconducting ($E_{\text{gap}} \sim 1\text{-}2 \text{ eV}$)**
- ✓ **Not centrosymmetric**
- ✓ **3m point group leads to non-zero d_{11} and e_{11} coefficients**

$$\begin{bmatrix} \varepsilon_{xx} \\ \varepsilon_{yy} \\ \varepsilon_{xy} \end{bmatrix} = \begin{bmatrix} d_{11} & 0 & 0 \\ -d_{11} & 0 & 0 \\ 0 & -d_{11} & 0 \end{bmatrix} \begin{bmatrix} E_x \\ E_y \\ E_z \end{bmatrix}$$



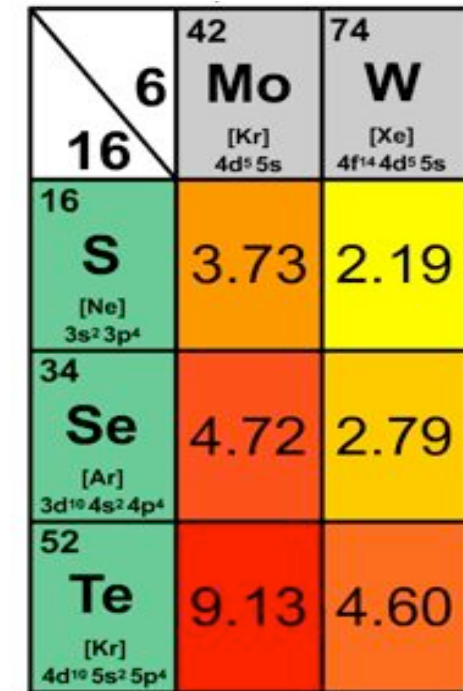
METHOD FOR DETERMINING PIEZOELECTRIC COEFFICIENTS



WE DISCOVER THAT A VARIETY OF TMDCS HAVE SIGNIFICANT PIEZOELECTRIC EFFECTS



Material	<i>Relaxed-ion coefficient</i>	
	$e_{11} (10^{-10} \text{ C/m})$	$d_{11} (\text{pm/V})$
h-BN	1.38	0.60
2H-MoS ₂	3.64	3.73
2H-MoSe ₂	3.92	4.72
2H-MoTe ₂	5.43	9.13
2H-WS ₂	2.47	2.19
2H-WSe ₂	2.71	2.79
2H-WTe ₂	3.40	4.60
Bulk α -quartz		2.3 (d_{11})
Bulk GaN (wurtzite)		3.1 (d_{33})
Bulk AlN (wurtzite)		5.1 (d_{33})



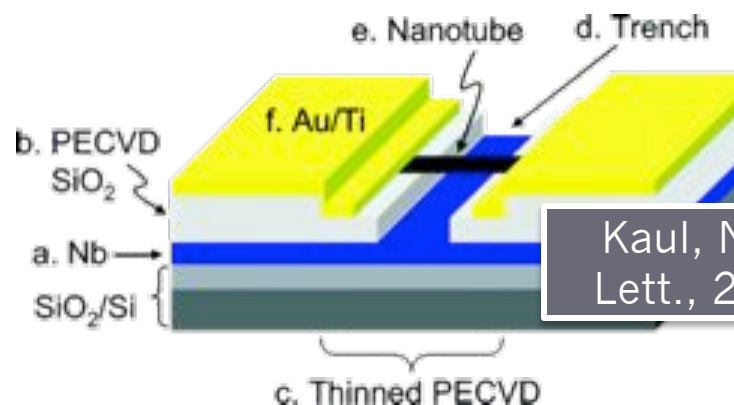
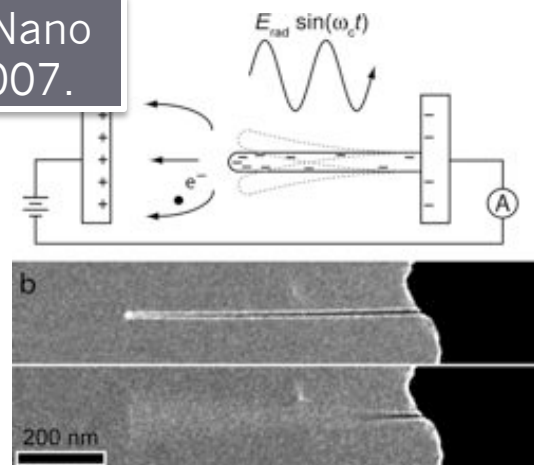
Piezo-coefficients of trigonal prismatic TMDC structures are comparable to bulk wurtzite structures

d_{11} values exhibit a periodic trend

K.-A. Duerloo, M. T. Ong, E. J. Reed., J. Phys. Chem. Lett. 3, 2871 (2012).

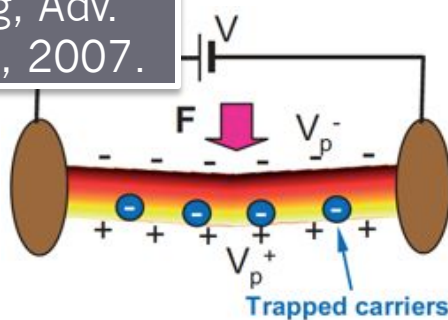
electromechanical nanotube devices

Jensen, Nano Lett., 2007.

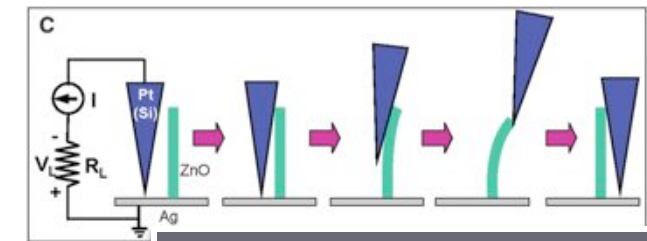
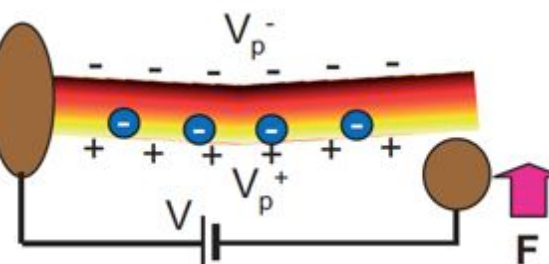


Kaul, Nano Lett., 2006.

Wang, Adv. Mater., 2007.



piezotronic nanowires

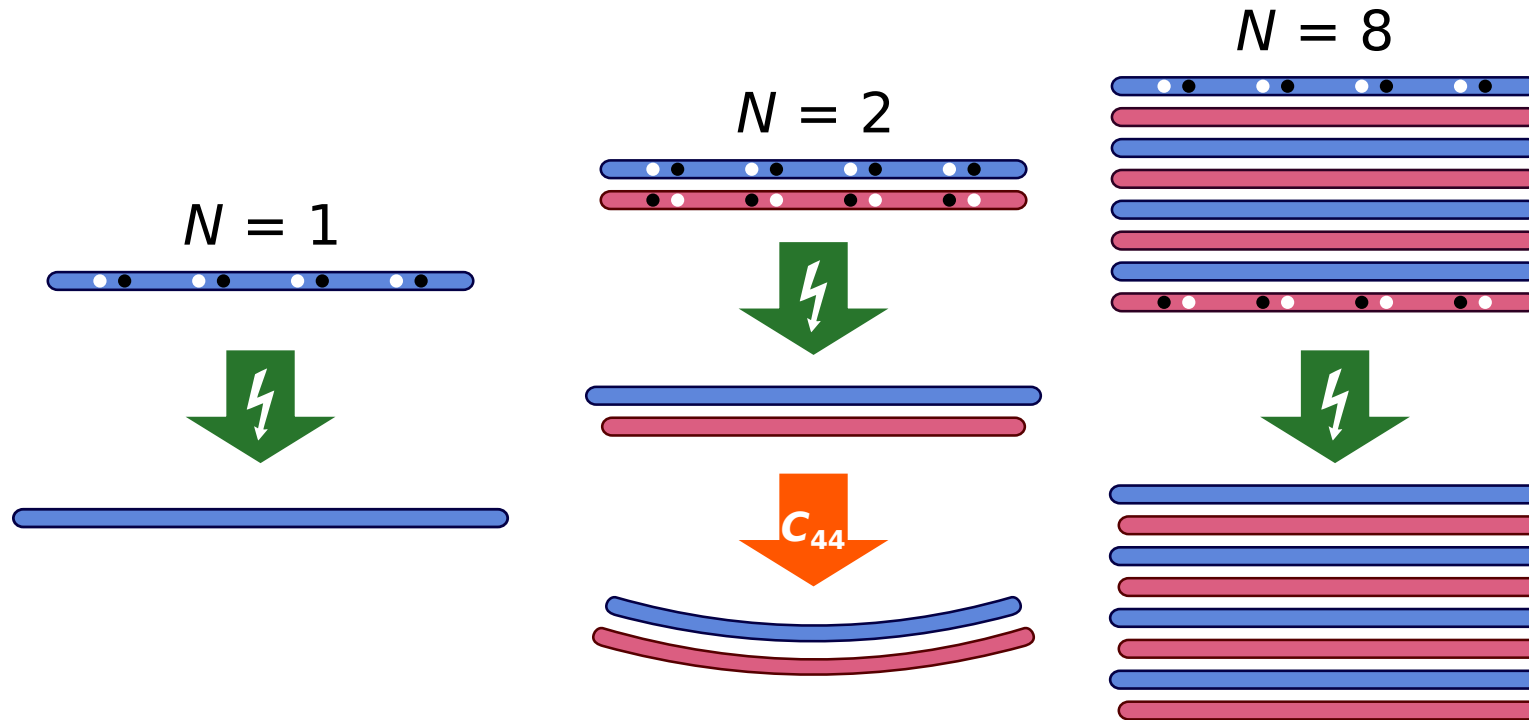


Wang, Science, 2006.

BULK TMDC CRYSTALS ARE NOT PIEZOELECTRIC



We find that TMDC monolayers are piezoelectric while their bulk host crystals exhibit an inversion center and are therefore not piezoelectric!



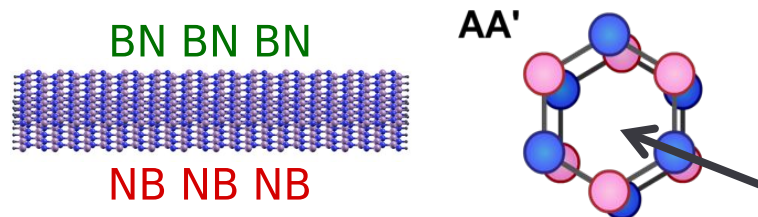
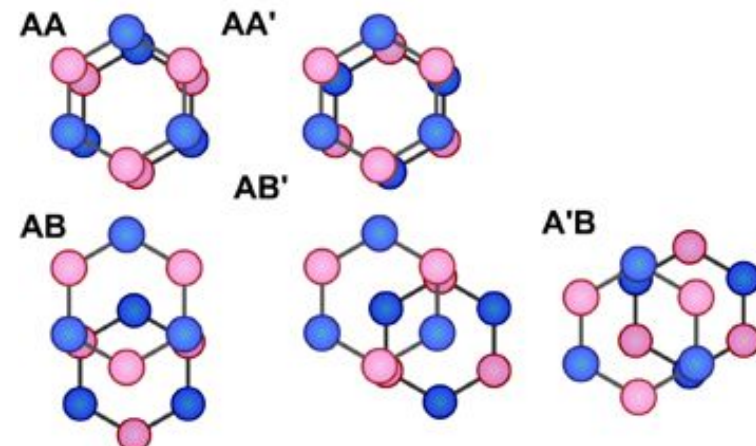
How does piezoelectricity change with the number of layers?
 Are there any novel types of electromechanical coupling in the few layer regime?

BILAYER BN EXHIBITS AN ELECTROMECHANICAL CURVATURE



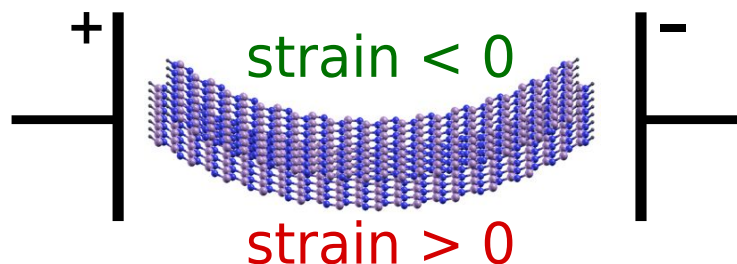
Bilayer BN can have a number of stacking sequences.

AA' is among the most energetically favorable and is found in the bulk structure.



inversion center
halfway between
layers:

NOT
PIEZOELECTRIC



Flexoelectric-type effect

$$\frac{\partial \varepsilon_{ij}}{\partial x_k} = \mu_{ijkl} E_l$$

$$\frac{2\varepsilon_{xx}}{h} = \kappa \approx \mu_{1131} E_1$$

↑
Inv. radius of
curvature

WE EMPLOY AN ELASTIC MODEL OF THE BILAYER



We have developed an elastic model that accounts for:

- In-plane elasticity of individual monolayers
- Out-of-plane curvature of the individual monolayers
- Piezoelectricity of the individual monolayers
- Interlayer sliding
- Interlayer cohesion

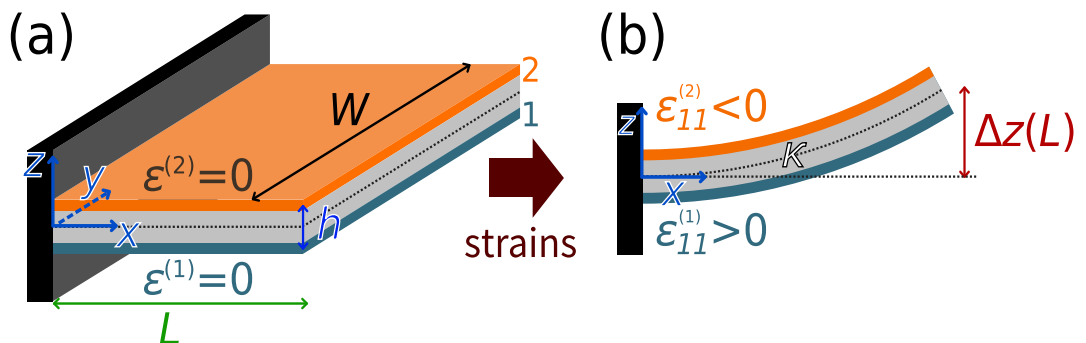
Equilibrium curvature:

$$\kappa_{\text{eq}} = \frac{2d_{11}E}{h_0} \cdot \lambda(L) \cdot \frac{1 - C_{12}/C_{11}}{1 + \frac{4D}{C_{11}h_0^2} + \frac{6D}{C_{44}^{\text{bulk}}h_0^2} L^{-2}}$$

With parameters computed using DFT:

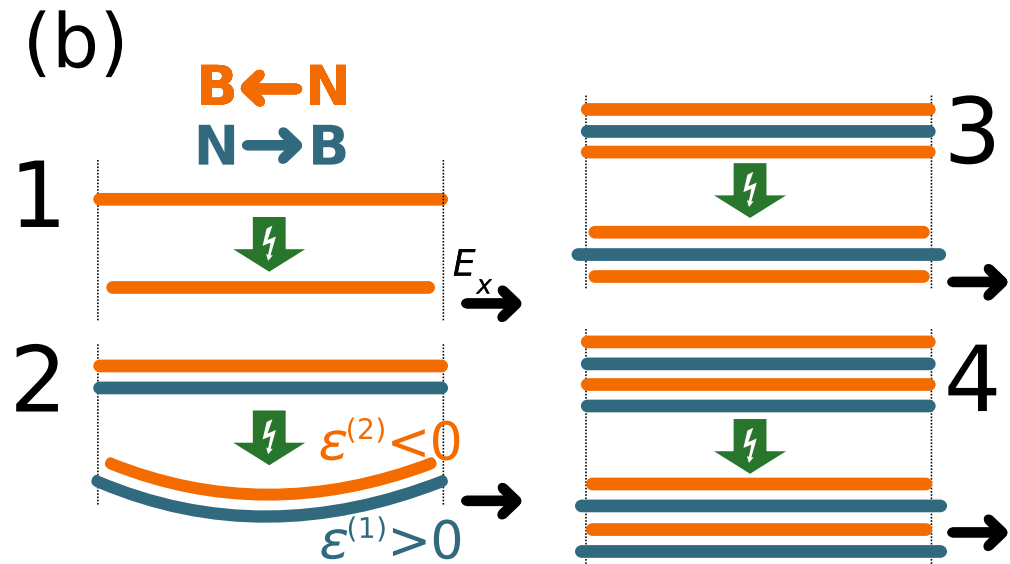
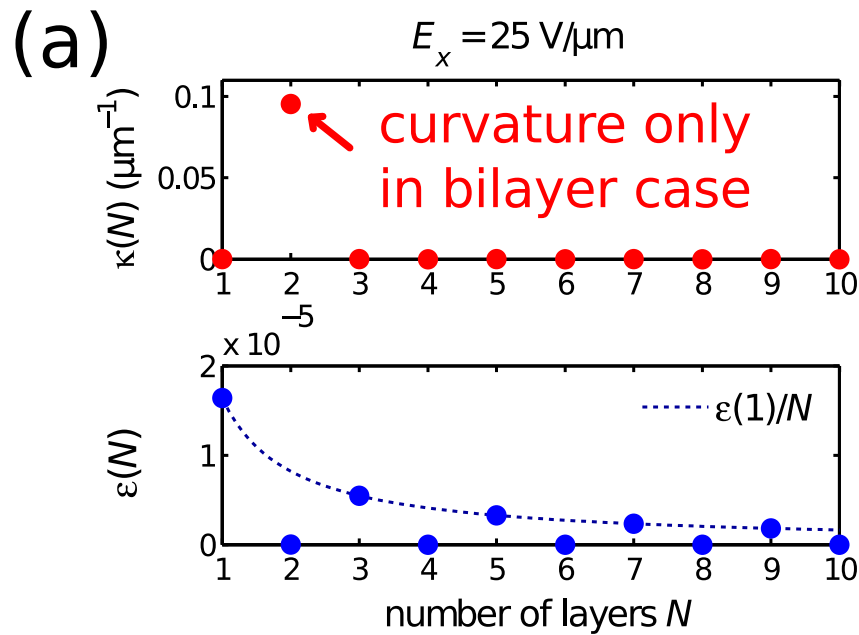
10 micron radius of curvature results from 25 V/ μ m field.

Comparable to CNT NEMS but with lower fields.



K.-A. Duerloo, E. J. Reed., Nano Letters (2013).

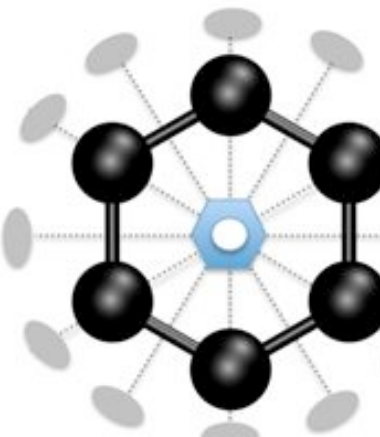
ELECTROMECHANICAL CURVATURE OCCURS ONLY FOR BILAYERS



- Our elasticity model predicts that appreciable curvature only occurs for bilayers.
- It is suppressed for 4-layer and higher even-layer structures due to the energy penalty for not maintaining coherence.

Graphene is not piezoelectric:

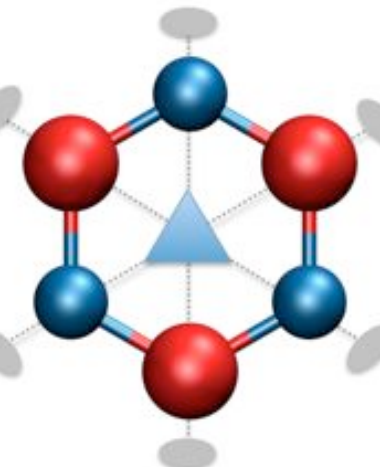
graphene



6/mmm

*Inversion symmetry =>
non-piezoelectric*

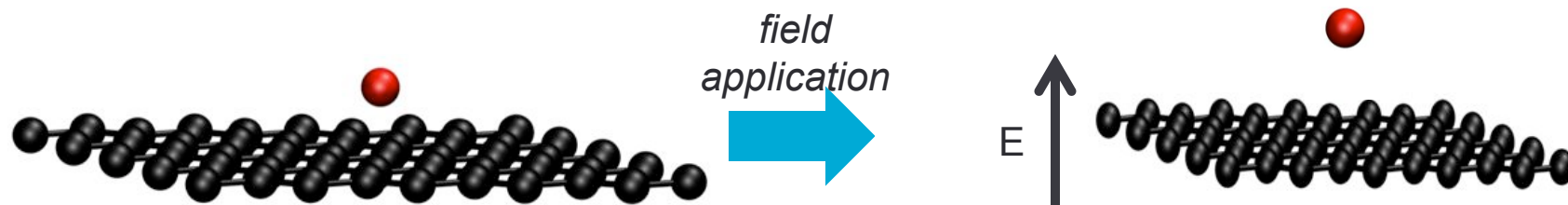
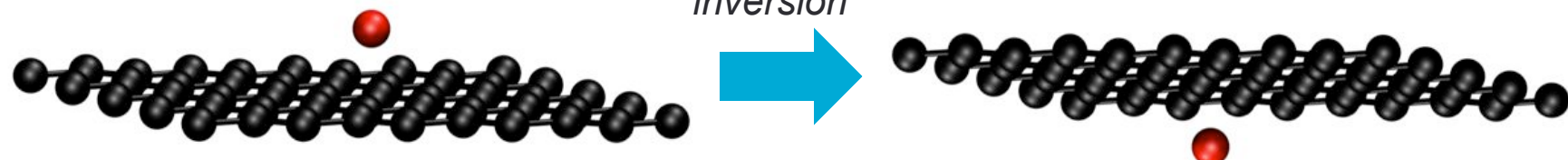
2D boron-nitride



32

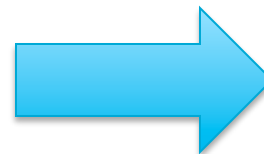
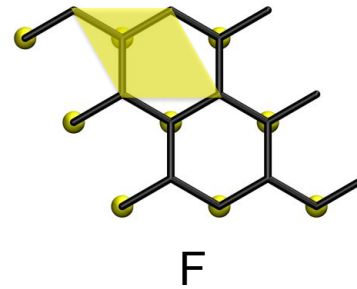
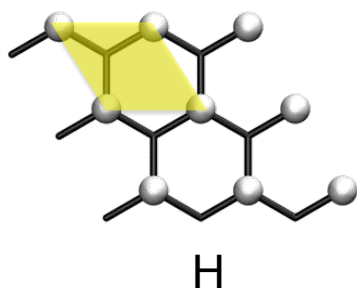
*No inversion symmetry =>
piezoelectric*

Can a non-piezoelectric material be made piezoelectric?

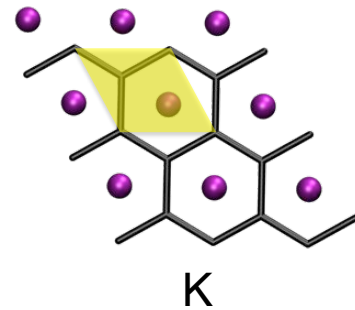
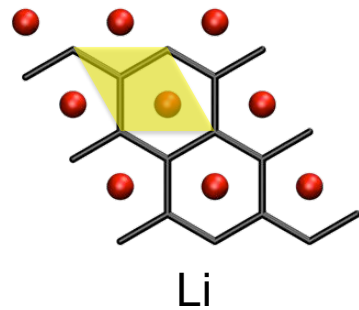


- Adatom adsorption gives rise to a locally broken inversion symmetry and a non-zero d_{31} and e_{31} coefficient coupling perpendicular fields to in-plane (equibiaxial) strain.
- Material is electrically insulating perpendicular to the plane.

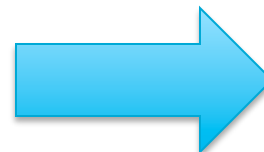
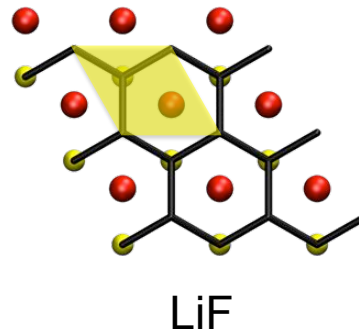
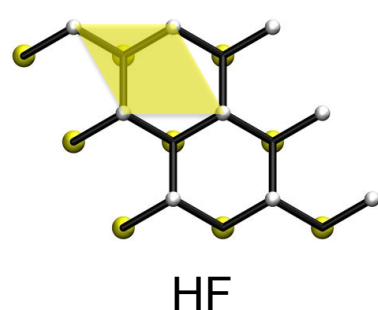
WE CONSIDER SEVERAL CASES OF ADATOM ADSORPTION



Single-sided and H and F over C atom sites.



Single-sided Li and K over “hole” sites.

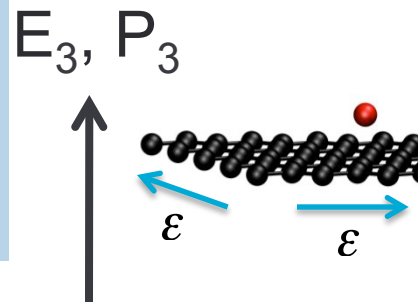


Two-sided adsorption, different atoms on each side.

DFT PIEZOELECTRIC CALCULATIONS GIVE VALUES SIMILAR TO 3D



The electric field of an applied gate voltage couples to equibiaxial strain ϵ .

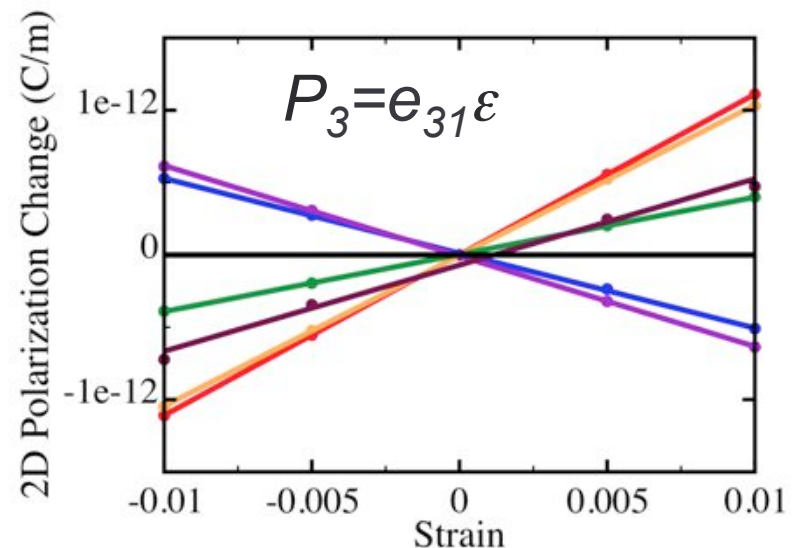
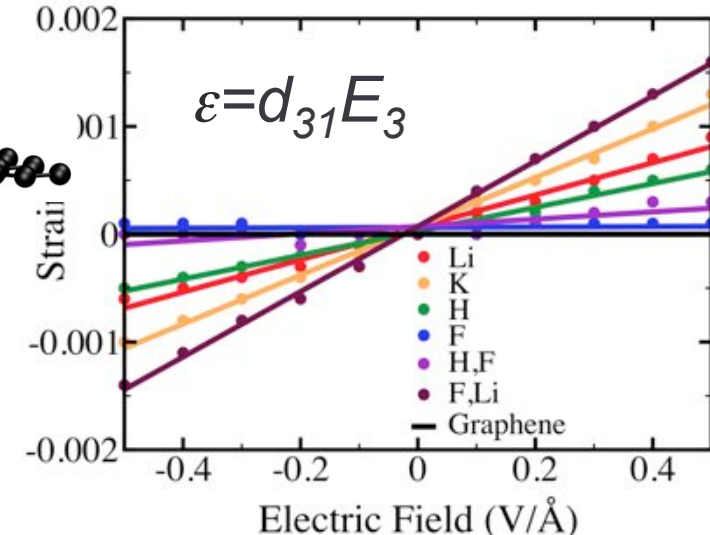


atom(s)	d_{31} (pm/V)	e_{31} (C/m)
Li	1.5×10^{-1}	5.5×10^{-11}
K	2.3×10^{-1}	5.2×10^{-11}
H	1.1×10^{-1}	2.0×10^{-11}
F	1.8×10^{-3}	-2.6×10^{-11}
H,F	3.4×10^{-2}	-3.1×10^{-11}
F,Li	3.0×10^{-1}	3.0×10^{-11}

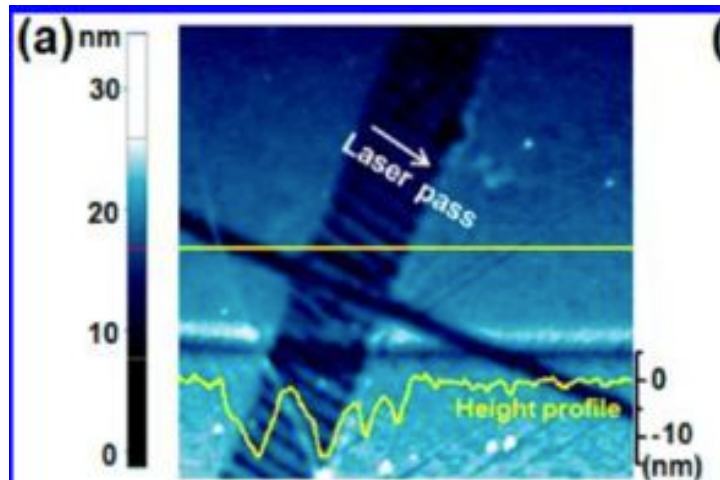
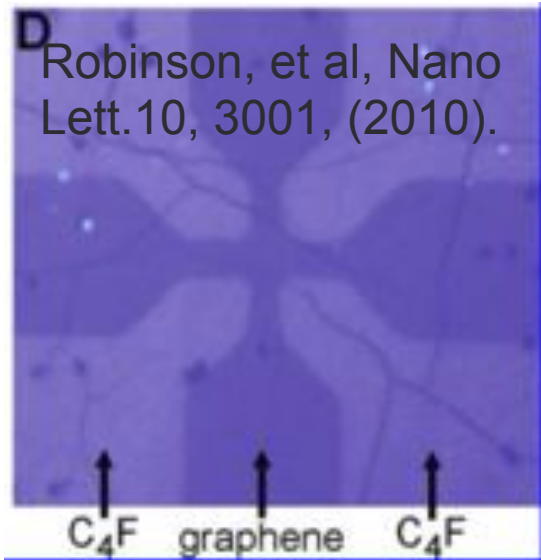
^aDoping with both F and Li give the largest d_{31} piezoelectric coefficient while doping with either Li or K gives the largest e_{31} piezoelectric coefficient.

d_{31} values for wurtzite 3D materials:
 BN: 0.33 pm/V
 GaN: 1.0 pm/V

Within factor of 3 of engineered 2D piezoelectric values.



SPATIAL CONTROL OF FLUORINATION HAS BEEN ACHIEVED



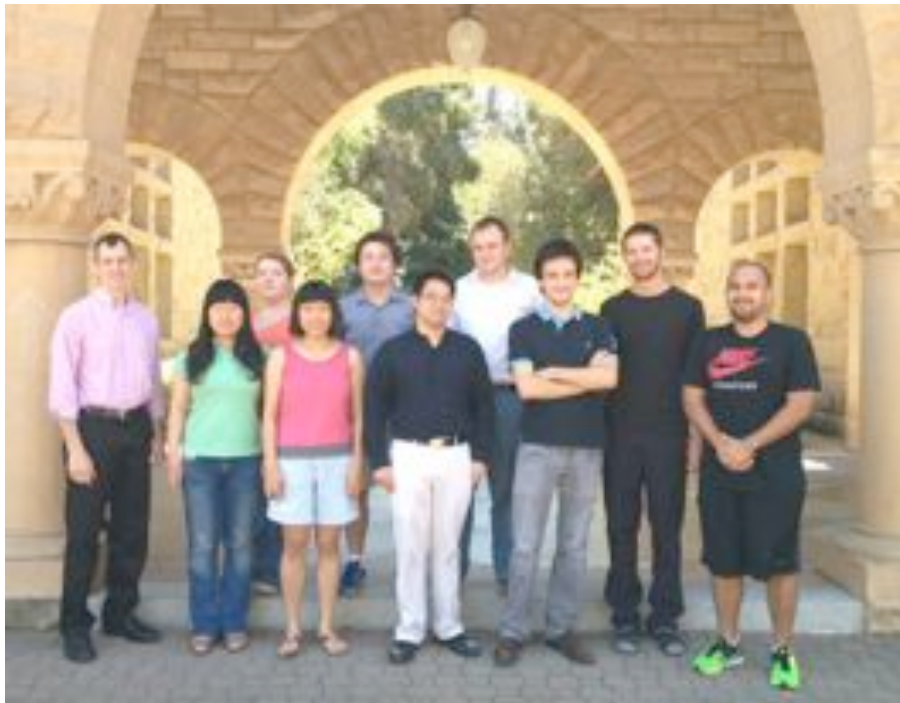
Lee, et al, Nano Lett. 12, 2374 (2012).

Spatial patterning of single-sided fluorine has been demonstrated using a photolithographic approach.

Spatial patterning of fluorine has also been achieved by laser-illumination of a fluorinated polymer.

Spatial patterning of adsorbed atoms suggests the potential for monolithic integration with other devices on-chip.

ACKNOWLEDGEMENTS



- Karel-Alexander Duerloo
- Mitchell Ong (now at LLNL)



This work is supported by:

- Army High Performance Computer Research Center (AHPCRC)
- DARPA
- National Energy Research Science Computing Center (NERSC)
- National Nanotechnology Infrastructure Network (NNIN)